Crustal structure and lateral variations in the Gulf of Mexico conjugate margins: From rifting to break-up

E. Izquierdo-Llavall, J.C. Ringenbach, F. Sapin, T. Rives, J.P. Callot

Version of Record: https://www.sciencedirect.com/science/article/pii/S0264817221005870
Manuscript_3d6279918a3634e084bea842bd57bccb

Crustal structure and lateral variations in the Gulf of Mexico conjugate margins: from rifting to break-up

Izquierdo-Llavall, E.[1,2], Ringenbach, J.C.[2], Sapin, F.[2], Rives, T.[2], Callot, J.P.[1]

[1] Université de Pau et des Pays de l'Adour, E2S UPPA, CNRS, TOTAL, LFCR, Pau, France ;

[2] TotalEnergies se, Structural Geology Department, CSTJF, Av. Larribau, 64000 Pau, France

Abstract

The Gulf of Mexico opened as a Late Triassic-Mid Jurassic continental rift that was first largely covered by the Mid-Jurassic Louann Salt and later split apart by a triangular-shaped oceanic crust. Salt in the Gulf of Mexico largely hampers the imaging and interpretation of underlying pre-salt and crustal geometries, which are fundamental for assessing the early kinematic evolution of the margin. To better define these deep geometries and their lateral variations, we built three seismic-based crustal-scale cross-sections across the Florida-Yucatan conjugate margins, in the areas where the Louann Salt is thinner. They were used, together with magnetic and gravity anomalies data, to build a crustal domains map for the study area. Cross-sections show a meaningful along-strike variation: the South Florida-East Yucatan area is characterized by a narrower rifted continental crust that evolves sharply to oceanic crust whereas in the North Florida and central-western Yucatan areas, the rifted continental crust is wider and the transition to the oceanic crust corresponds to a narrow magmatic or exhumed mantle domain. Bulk continental crust extension was determined using the area balancing method. Estimated horizontal extension values vary from a minimum of ~120 km in the South Florida-East Yucatan conjugate to a minimum of ~240 km in the North Florida-Central Yucatan conjugate, being systematically larger in the northern margin. Based on our observations and considering previous models, we propose that the study area evolved from an early rift involving magmatism, to a magma-poor margin, with continental break-up (OCT formation) being characterized by mantle exhumation and associated magmatism along the North

Florida and central-western Yucatan areas. As in other analogues such as the Gulf of Guinea, the thick evaporite deposited during the late rift, while mantle was being exhumed.

Keywords: Gulf of Mexico; rifted margins; crustal-scale cross-sections; ocean-continent transition; rifting; break-up; continental crust extension

1. Introduction

Lateral variations in basement faulting, syn-rift stratigraphy, magmatic contribution and width of structural domains have been described in numerous margins distributed worldwide, including the Argentina-Uruguay (Franke et al., 2007; Soto et al., 2011; Chauvet et al., 2020), the South-West African (Koopmann et al., 2014), the Norwegian-Greenland Sea (Faleide et al., 2008; Tsikalas et al., 2008; Péron-Pinvidic and Osmundsen, 2018; Gernigon et al., 2019), the Iberia-Newfoundland (Péron-Pinvidic et al., 2007; Sutra et al., 2013; Pereira et al., 2017), the Great Australian Bight (Espurt et al., 2012), the Angola-Gabon (Unternehr et al., 2010; Epin et al., 2021), the Labrador Sea (Keen et al., 2018; Gouiza and Paton, 2019), the South China Sea (Fan et al., 2019; Zhao et al., 2020) and the Nova Scotia (Lau et al., 2019) margins.

Lateral variations between the different segments forming these margins are either diffuse or sharp and occur at various scales, from tens to hundreds of kilometers (Turner et al., 2003). In margins where magmatic contribution is important (such as the Argentina-Uruguay or the South-West African margins; Hinz et al., 1999, Koopmann et al., 2014), lateral variations commonly relate to along-strike variations in the architecture, volume and width of seaward dipping reflectors (SDR) that are accompanied by lateral changes in the thickness and distribution of post-rift sediments (Franke et al., 2007; Chauvet et al., 2020). In margins where magmatic contribution is more limited (the Mid- Norwegian-NE Greenland, the Angola-Gabon, the Iberia-Newfoundland or the Great Australian Bight margins; Sutra and Manatschal,

2012; Espurt et al., 2012; Pereira et al., 2017; Péron-Pinvidic et al., 2017; Péron-Pinvidic and Osmundsen, 2018; Epin et al., 2021), lateral changes in the rift architecture mostly refer to the width, structure and asymmetry of the thinned continental crust and the overlying syn- and post-rift stratigraphy. Along-strike changes in the width of the exhumed mantle (Espurt et al., 2012; Sutra et al., 2013) or the occurrence of syn-rift magmatism (Eddy et al., 2017; Pereira et al., 2017) have also been reported and correlated to lateral changes in margin asymmetry (Pereira et al., 2017).

The analysis of lateral changes in rifted margins is of key importance for the understanding of their thermal and kinematic evolution because they inform about different processes such as (i) the influence of inherited structures (Jammes and Huismans, 2012; Peron-Pinvidic et al., 2017; Duretz et al., 2016; Zhao et al., 2020), (ii) the thermal and compositional state of the lithosphere, controlling its rheology (Huismans and Beaumont, 2008; Liao and Gerya, 2014; Sapin et al., 2021), (iii) the lateral variation in extension rates or total extension values (Rey et al., 2009; Brune et al., 2016; Tetrault and Buiter, 2018), (iv) the migration of rifting prior to breakup (Pereira and Alves, 2011) or (v) the lateral variation in rifting obliquity (e.g., Antobreh et al., 2009; Zwaan et al., 2016).

Similarly to the aforementioned margins, the Gulf of Mexico conjugate margins also display along-strike variations in the crustal architecture (Pascoe et al., 2016; Pindell et al., 2016; Ewing and Galloway, 2019). Continental rifting in the Gulf of Mexico initiated during the Late Triassic (Salvador, 1987; Frederick et al., 2020 and references therein) and continued up to the onset of oceanic spreading in Late Jurassic times (Pindell et al., 2016; Lin et al., 2019; Hudec and Norton 2019 among others). Rifting resulted in the development of a set of contiguous Triassic and Jurassic sub-basins that were largely covered by a thick Mid-Jurassic salt unit (the Louann Salt; Peel et al., 1995; Fredrich et al. 2007; Galloway, 2008; Hudec et al., 2013). This salt has been estimated to have been up to 4 km in original thickness (Peel et al., 1995; Galloway, 2008; Hudec et al., 2013; Rowan, 2018), with subsequent salt tectonics substantially hindering

the seismic imaging of underlying syn-rift geometries, which remain largely unsolved. Continental crust geometries soling syn-rift basins have been described along individual, deep seismic reflection (Pindell et al., 2014, 2018; Pascoe et al., 2016; Rowan, 2018; Snedden and Galloway, 2019) and refraction profiles (Christeson et al., 2014; Van Avendonk et al., 2015; Eddy et al., 2014, 2018), but further efforts are required for the integration of these 2D observations into regional-scale maps assessing the along-strike variations in the margin.

The objective of the present work is to describe crustal and syn-rift geometries in the Gulf of Mexico and to characterize their lateral variations, aiming to better define the evolution of the margin and the processes governing it. For this purpose, we have constructed three crustal-scale cross-sections of conjugate segments based on deep and depth-migrated seismic reflection data (Fig. 1). Cross-sections extend across the eastern and south-central Gulf of Mexico where Mid-Jurassic salt is thinner and consequently pre-salt and crustal features are better imaged (salt tectonics across them is minor to moderate and its discussion is beyond the scope of this work). The seismic-based cross-sections allowed us to define the location of crustal domains boundaries that, combined with gravity and magnetic anomaly data, have been laterally correlated to build regional crustal domains and syn-rift distribution maps. The cross-sections were restored and used to calculate continental crust extension values in the Yucatan and Florida margins. Lateral variations in both crustal geometries and continental stretching values are identified and their implications for the early history of the margin are analyzed and discussed in the light of observations derived from other natural case studies.

2. Geological Framework

The present-day structure of the Gulf of Mexico results from a long-lasting evolution including continental rifting (Triassic to Middle Jurassic) and seafloor spreading stages (onset of oceanic spreading in the Late Jurassic until Berriasian-Valanginian times, Pindell et al., 2016, 2021; Lin et al., 2019). Oceanic

spreading was accompanied and followed by Late Jurassic and Cretaceous–Cenozoic sedimentation. From Coniacian times, the sedimentary evolution of the Gulf of Mexico was largely controlled and impacted by the convergence along the western margin of the North American plate (Fig. 2; Feng et al., 1994 among others).

Continental rifting in the Gulf of Mexico area was driven by the relative motion between the North America plate and the Yucatan and Florida blocks (Pindell, 1985; Marton and Buffler, 1994, among others). Early rifting began in the Late Triassic and partly dismantled the Ouachita-Appalachian orogen, formed during the Carboniferous as the result of the collision between North America and Gondwana (Pindell and Dewey, 1982; Pindell, 1985; Dallmeyer, 1989; Horton et al., 1989). Structural inheritance along the Carboniferous orogen exerted a strong control on the development of the Late Triassic rift basins that were filled by the Eagle Mills formation (Fig. 2). This stratigraphic unit is mostly made of siliciclastic sediments in the South Georgia Basin (SGB in Fig. 1a), the onshore East Texas, Louisiana and Arkansas areas (the Texas-Louisiana-Arkansas Basin; Salvador, 1987, 1991, Wood and Benson, 2000; Heffner, 2013) and the onshore Mexico (Lawton, 2018). Sedimentation of the Eagle Mills formation was partly accompanied and followed by intense igneous activity in the Yucatan (Lawton et al. 2009; Godínez-Urban et al., 2011a, b), South Georgia Basin (Frederick et al., 2020; Heffner, 2013) and South Florida areas (Pollastro et al., 2001; Wiley, 2017 and references therein), with abundant Early Jurassic lava flows, dykes and sills (May, 1971; Heatherington and Mueller, 2003; Mickus et al. 2009; Fig. 2). This Early Jurassic magmatism in the Gulf of Mexico was in part coeval to the thick basalt flows of the Central Atlantic Magmatic Province (CAMP, ~200 Ma, Withjack et al., 1998; Marzoli et al., 2011) and occurred under a general context of continental crust stretching and thinning that culminated with mantle exhumation in some parts of the Gulf of Mexico margin (Rowan, 2018). In areas south of the Appalachian fold-and-thrust belt, Late Triassic-Early Jurassic rifting took place under a general NW-SE extensional stress field (Pindell and Kennan, 2009; Eddy et al., 2014; Nguyen and Mann, 2016; Lin et al.,

2018; Pindell et al., 2021) and resulted in the formation of NE-trending basins in the United States onshore (the South Georgia and Texas-Louisiana-Arkansas Basins) and the West Florida offshore (see early rift, phase-1 structures in Fig. 1a). The latter have been interpreted to result from a NW-directed, continental crust extension attaining a minimum of 320 km (Pindell et al., 2015, 2021). Oblique, E-W to NW-SE trending early rift depocenters and extensional faults have also been reconstructed from the correlation of seismic lines in the West Florida offshore (Apalachicola Basin in Fig. 1a, Liu et al., 2019; Storey, 2020; Frederick et al., 2020). These basins were likely coeval to the formation of a thick, NE-trending (present-day coordinates) depocenter identified in central and West Yucatan (see location in Fig. 1a, Miranda-Peralta et al., 2014). The Louann Salt basin formed in the latest stages of continental crust extension and/or during mantle exhumation and was later split apart during oceanic spreading (Pindell, 1985; Bird et al., 2005; Hudec et al., 2013; Rowan, 2018; Hudec and Norton, 2019; Pindell et al., 2014, 2021). Louann Salt ages (Fig. 2) are constrained by: (i) recent $^{87/86}$Sr analysis (Pulham et al. 2019; Snedden and Galloway, 2019; Pindell et al., 2019, 2020) that reveal an age close to 170 Ma (Bajocian) and (ii) the first paleontological dating in the post-salt sequence that indicates an Oxfordian age for the units above the salt (Olson et al., 2015; Snedden and Galloway, 2019). Halite is the dominant mineral phase in the allochthonous Louann units (Fredrich et al., 2007) although anhydrite has been drilled by wells in the north-eastern Gulf of Mexico (Snedden and Galloway, 2019 and references therein). In this area, seismic data point out that autochthonous halite laterally and vertically grades to anhydrite (Tew et al. 1991; Snedden et al., 2018; Snedden and Galloway, 2019) and other carbonate and detrital units (the so-called Sakarn series, Rives et al., 2019; Fig. 2) which were deposited in the northeastern Gulf of Mexico contemporaneously to evaporite precipitation further north and west (Rives et al., 2019).

The Louann Salt is overlain by fluviatile and aeolian units (Norphlet) and marine carbonates (Smackover, Fig. 2). This sequence recorded the evolution of the basin from arid, restricted conditions (Galloway 2008; Hudec et al., 2013; Peel, 2019) to near-normal marine salinity conditions during the middle and

upper Oxfordian. Oceanic crust accretion began in Late Jurassic times (Pindell and Kennan 2001, 2009; Deighton et al., 2017; Hudec and Norton, 2019) and split apart the previously developed continental rift. It was coeval to the counter-clockwise rotation of the Yucatan block around a single (Pindell and Dewey, 1982; Pindell, 1985; Nguyen and Mann, 2016; Minguez et al., 2020 among others) or successive rotation poles (Pindell and Kennan, 2009; Pindell et al., 2016; Pindell et al., 2021) located in western Cuba and the eastern Gulf of Mexico. Continental rifting during this rotation (phase-2 rift) is defined by extensional structures running parallel to the continent-ocean boundary. These late extensional faults are NW-striking in the south-eastern Gulf of Mexico, where they trend highly obliquely to early rift faults (Pindell et al., 2015, 2021).

Sedimentation during the latest Jurassic and the Early and Mid-Cretaceous time interval was dominated by carbonates with development of widespread Mid-Cretaceous platform margin reef systems (Snedden and Galloway, 2019), in an open, normal-salinity marine basin. The latest Jurassic to Mid-Cretaceous sedimentary sequence recorded an increase of subsidence and sedimentation rates with respect to the underlying Jurassic. This produced the loading and seaward tilting of the Louann Salt over the continental margin and triggered the gravity gliding of the Jurassic interval in the north-eastern Gulf of Mexico (Pilcher et al. 2014; Rives et al., 2019) and the Yucatan domain (Steier and Mann, 2019).

In the Late Cretaceous, the input of clastic sediments into the western Gulf of Mexico basin increased dramatically. Sandstones were deposited into the deep basin during the Cenomanian-Turonian (Snedden et al., 2016) and were later confined to shelf and shorelines during Campanian-Maastrichtian (Haq, 2014). Finally, Cenozoic sedimentation was characterized by the development of thick depocenters along the western and northern Gulf of Mexico where Cenozoic sediments were supplied by continental rivers sourced by the reliefs surrounding the basin (Galloway et al. 2011; Snedden and Galloway, 2019).

3. Geometry of the conjugate margins: Insights from deep seismic reflection profiles

For this study, two approximately conjugate cross-sections were built across the Florida-Yucatan rifted margins (see restoration in Fig. 1b). They are completed by a third cross-section running through the western Yucatan domain whose conjugate part is approximately located along the trace of the seismic refraction profile Gumbo-2 (Eddy et al., 2018), offshore Texas (Fig. 1). The easternmost cross-section is referred in the text as the South Florida-East Yucatan cross-section whereas the central and western profiles are hereinafter referred to as the North Florida-Central Yucatan and West Yucatan cross-sections, respectively. Cross-sections are E-W to NE-SW-striking in the Florida margin and NW-SE-striking in the Yucatan domain (Fig. 1). They are perpendicular or sub-perpendicular to the limit of the oceanic crust (LOC in Fig. 1a) and to late rift (phase-2) structures in the deep offshore. Nevertheless, they have a variable orientation with respect the early (phase-1) faults, being highly oblique (~25º) in the South Florida-East Yucatan cross-section and moderately oblique (~50-60º) to perpendicular in the North Florida-Central Yucatan and West Yucatan profiles respectively.

3.1. Datasets

Cross-sections in this work are tied to deep penetrations and pre-stack depth-migrated seismic reflection profiles shot and processed by ION (GXT Florida Span and Gulf Span surveys). They allow interpreting sub-salt and crustal-scale geometries in the Yucatan and Florida sectors. Nevertheless, deep seismic imaging in the north-central Gulf of Mexico is largely obscured by the presence of the thick and deformed Louann Salt which prevented the completion of the northern conjugate cross-section in West Yucatan. Besides seismic reflection data, crustal thicknesses and first-order crustal geometries in the study area are also constrained by seismic refraction profiles in the northern Gulf of Mexico (see location of GUMBO profiles in Fig. 1, Christeson et al., 2014; Eddy et al., 2014, 2018; Van Avendonk et al., 2015) whereas the map view of regional-scale gravity and magnetic anomaly data (Maus et al., 2009;

Bonvalot et al., 2012; Sandwell et al., 2014; Pindell et al., 2016; Bain et al., 2019) provide additional information on the trends and the along strike extent of crustal-scale features. Main litho-stratigraphic boundaries and sedimentary thicknesses are partly defined from available wells that are mostly located in the Florida platform area (see well location in Fig. 1a)

3.2. Seismic interpretation strategy

The seismic-based cross-sections presented in this study integrate the interpretation of both, (i) the syn- and post-rift sedimentary sequence in Florida and Yucatan margins and (ii) the deepest crustal structures underlying them. The boundary between the syn- or post-rift sediments and the continental crust corresponds to the top continental basement horizon. In the Florida platform, the top of the basement is locally drilled by wells (Figs. 1, 4) that found Early Paleozoic granitic batholiths and associated volcanic rocks (see well data compilation in Lin, 2018). The top continental basement was mostly defined by the lateral extension of these well data through the Florida margin. In areas where we could not propagate well data, the top continental basement horizon was generally identified by a high amplitude reflection at the base of syn-rift packages (Fig. 3a, b, c), locally obscured by igneous intrusions/flows. In the oceanic crust, the top basement horizon was easily recognized along seismic reflection profiles, marked by the strong contrast between reflective, well-bedded sediments and the transparent/chaotic upper oceanic crust (Fig. 3e).

Overlying the continental and oceanic basements, the sedimentary sequence has been divided into six main units, from the base to the top (Figs. 2, 3): the pre-Louann Salt sequence, the Louann Evaporites, the Jurassic post-salt, the Cretaceous, the Paleogene and the Neogene. Based on the previously described age constraints (see section 2, Fig. 2), the Louann Salt could extend from Bajocian to Callovian times meaning that the post-salt Jurassic represents mainly the Upper Jurassic whereas the pre-salt can include Lower Jurassic up to Aalenian units and can be as old as the Eagle Mills unit (Late Triassic in age).

The boundaries between the Jurassic, the Cretaceous, the Paleogene and the Neogene are well-tied in the Florida Platform (Figs. 1, 7) and have been extended through the oceanic crust to the Yucatan domain thanks to their distinctive seismic character. The Louann Salt boundaries have been initially defined across the central and western cross-sections where mobile halite is probably dominant, represented by transparent to chaotic seismic facies (Fig. 3b, c). From these sections, salt boundaries have been extended to the East where, according to previous interpretations (Snedden et al., 2018; Snedden and Galloway, 2019), evaporites are less mobile and anhydrite is locally present (it is imaged as high amplitude, continuous reflections and drilled by wells, Snedden et al., 2018; Snedden and Galloway, 2019).

Regarding the pre-salt units, we differentiated (where possible) the different forming sequences (early and late syn-rift and sag sequences). Geometrical and seismic facies criteria were used and special attention was paid to the cross-cutting relationship between horizons and basement faults. At crustal scale, two main surfaces have been defined: the base of both continental and oceanic crusts (i.e., the Moho) and the boundary between the upper and the middle-lower crust (i.e., the Conrad). The Moho was identified as a high amplitude reflection that is normally continuous and well-imaged along the thinned continental crust and the oceanic crust (at depths ranging between 25 and 15 km; Fig. 3a, b, c, e). Underneath the proximal continental crust, the Moho was discontinuously identified as a roughly flat, strong reflection at depths varying between 35 and 40 km. Where possible, the boundary between the upper and the middle-lower crust was also defined as the transition between an upper, more transparent crust and an underlying layered crust displaying high-amplitude reflections. This boundary is identified to correspond to a major décollement on top of which major rifting faults are rooting (Fig. 3a, c). This boundary is clearer across the distal continental crust, but more diffuse and interpretative in the proximal margin. In the transition between the continental and the oceanic crust, high amplitude, discontinuous reflections have been frequently identified and interpreted as magmatic additions

possibly representing extrusives, intrusives (sills and dykes) or magmatic underplating (e.g., Geoffroy et al., 2015, among others; see Fig. 3d).

3.3. Crustal-scale cross-sections of the conjugate margins

3.3.1. The eastern cross-section: South Florida - East Yucatan

The South Florida- East Yucatan cross-section (Fig. 4) is highly oblique to early rift structures and runs along a NE-trending basement high in West Florida (the Tampa Arch, see Fig. 1a) underlain by ≥ 30km –thick continental crust (Fig. 4). Rifting in the cross-section concentrates along a 100-150 km-wide zone where the continental crust shows a wedge shape.

In the ≥ 30km –thick continental crust, the high amplitude reflection marking the Moho is discontinuously observed at an approximately constant depth of 36 km in both the South Florida and East Yucatan margins. In this crustal domain, the top basement is encountered by wells at a depth of 3-3.5 km in the central part of the Florida platform (Fig. 4) and it is interpreted to deepen up to a maximum of approximately 5 km at the eastern boundary of the South Florida cross-section whereas it remains at a constant depth of 4-5 km in the East Yucatan margin. The basement is overlain by flat-lying sedimentary packages mostly including Cretaceous and Cenozoic units (wells in the Florida platform indicate that the Jurassic is locally absent, Fig. 4), with sedimentary thicknesses varying between 2-4 km and 3-5 km in the Yucatan and Florida margins respectively. The boundary between the upper and the middle-lower crust is inferred to be located at an approximate depth of 15 km, roughly corresponding to the transition to seismic velocities > 6.5 km/s in the seismic refraction profile Gumbo-4 which is located at an average of ~ 250 km to the North (Christeson et al., 2014, see location in Fig. 1).

The area where rifting concentrates (Figs. 4, 5, 6) is characterized by the general, oceanward deepening of the top continental basement and the progressive shallowing of the Moho, which results in the

thinning of the crust from ≥ 30km up to a minimum value of ~ 5 km at the limit of the continental crust (LCC). The crust is affected by an assemblage of doubly-vergent extensional faults (Fig. 5, 6). They branch at depth into an intra-crustal décollement probably located at the upper/middle-lower crust transition (see decoupled domain in Figs. 5, 6), except in the distalmost portion of the continental margin, where faults traverse the whole continental crust (i.e., they are coupled with the upper mantle; see coupled domain in Fig. 5). Seismic reflections in the lower crust describe sigmoidal geometries (Figs. 5 and 6) that can be interpreted as markers of a ductile shearing mechanism (following Clerc et al., 2018; Sapin et al., 2021). Basement faults in the rifted crust are related to syn-tectonic sedimentary wedges that reach a maximum thickness of 3-4 km. The syn-tectonic sequence forming these wedges includes an upper, higher reflectivity package and a lower, low reflective or transparent unit that correlates laterally to the Louann Salt. The sequence representing the lateral equivalent of the Louann Salt in the East Yucatan-South Florida cross-section is fault-bounded and shows reduced to no salt mobility. Similar geometries are depicted by Snedden and Galloway (2019) on seismic profiles in the eastern Gulf of Mexico where a mixture of anhydrite and halite is interpreted and drilled by wells. The syn-rift package is overlain by a thin Jurassic and a thicker Cretaceous and Cenozoic sequence that onlaps onto the older units. Onlaps are well-imaged in the East Yucatan margin where this stratigraphic boundary (indicated as the break-up unconformity, BKU in Fig. 4) separates syn- and post-rift deposits at the entire margin scale.

The oceanic crust is formed by a lower reflective and an upper transparent unit (Fig. 3e, 4). The transition between the continental and the oceanic crust is sharp (the LCC and the limit of the oceanic crust, LOC, overlap, Figs. 5, 6) and none of the typical geometries of exhumed mantle are identified, neither along the East Yucatan nor along the South Florida margins. The strong reflections identified underneath the continental and the oceanic Moho (Fig. 4, 5, 6) may indicate magmatic underplating at the continent-ocean boundary instead. The top of the oceanic crust is located at an average and almost constant depth of ~ 10 km. It is largely un-faulted except in the central part of the cross-section where a

symmetric graben, bounded by NE and SW dipping faults coincides with the position of the extinct mid oceanic ridge (MOR in Fig. 4), as identified by magnetic and gravity anomalies (gravity low from Lin et al., 2019), and on seismic velocity data as well (decrease in crustal seismic velocities in Christeson et al., 2014). The oceanic Moho is marked by a rugose, strong reflection that is found at an average depth of ~ 19 km, although it deepens underneath the mid-oceanic ridge where it attains a maximum depth of ~ 22 km. The average thickness of the oceanic crust (out of the extinct mid-oceanic ridge domain) is ~ 9 km.

3.3.2. The central cross-section: North Florida - Central Yucatan

The North Florida-Central Yucatan cross-section (Fig. 7), is moderately oblique to perpendicular to early rift (phase-1) structures. In West Florida, it runs along an E-W to NW-SE-trending basin (the Apalachicola basin, Fig. 1a) which is oblique to the regional NW-SE extension in early rifting stages (Pindell et al., 2021 and references therein). A > 30 km-thick crust is preserved at the outer limits of the cross-section (Fig. 7) where the Moho is imaged at an approximate depth of ~ 40 km and ~ 37-39 km in the North Florida and Central Yucatan margins respectively, the top basement being flat at a depth of 5 to 6 km.

In the rifted continental crust, the Moho shows an undulated geometry and a progressive basinward shallowing and crustal thicknesses decrease up to a minimum of 1-2 km at the ocean-continent transition (OCT, Figs. 8, 9). Crustal geometries differ in the North Florida and central Yucatan margins. In the central Yucatan margin, the Moho shallows along 200 km and the top basement remains flat and un-faulted in the Yucatan platform but it is faulted and progressively deepens in the deepest offshore. As in the South Florida-East Yucatan cross-section (Figs. 5, 6), faults are arranged into a coupled and a decoupled domain (Figs. 8), with related syn-rift units being considerably thicker in the central cross-section. The decoupled domain is characterized by dominantly landward dipping (i.e., SE-dipping) faults that branch at depth into a main décollement likely located at the transition between the upper and the lower-middle crust, whereas in the coupled domain faults are NW-dipping and traverse the whole crust.

The continental crust is well-imaged in the seismic reflection profile (Fig. 8) that allows identifying the limit between the upper and the middle-lower crust at an approximate depth of 12 to 16 km. Syn-tectonic units in the decoupled rift include high reflectivity packages defined by high amplitude, locally discontinuous, reflections that suggest the presence of abundant magmatic elements. They vertically and laterally grade into less reflective or semi-transparent units of probable sedimentary nature. The magmatic-like units are abundant in the decoupled domain where they are overlain and interbedded within sedimentary-like units, the latter being dominant in the coupled domain. From the distribution of these units, a progressive oceanward migration of faulting and related syn-tectonic sedimentation is inferred (as widely suggested in other rifted margins worldwide, Ranero and Perez-Gussinye, 2010; Péron-Pinvidic et al., 2019 and references therein). Basement faults are older in the decoupled domain and younger in the coupled rift where they locally cross-cut the whole pre-salt sedimentary sequence (i.e., the younger pre-salt package is un-faulted in the decoupled domain but small, fault-controlled thickness variations are inferred for this unit in the coupled rift area). The Louann Salt overlies this unit. Its base dips gently (~ 3º) to the North and remains largely un-faulted over the decoupled domain although it is slightly offset by some of the basement faults in the distalmost continental crust. The sedimentary package overlying the salt consists of a thick Mesozoic and Cenozoic sequence that is deformed by the gravity-induced gliding of the sediments over the evaporites (Steier and Mann, 2019; Hudec and Norton, 2019).

Moho, top basement and syn-rift geometries are significantly different in the North Florida margin (Figs. 9 and 10) where two extended crust domains can be distinguished: (i) an older, proximal rift, located underneath the Florida platform (i.e., the Apalachicola basin, Fig. 1a) and (ii) a younger, distal rift in the Florida deep offshore. In the proximal rift (Fig. 9), the Moho is interpreted to shallow up to ~28 km, defining a thinned crust area where pre-salt units were deposited. These pre-salt units reach a maximum thickness of 7-8 km and, based on seismic reflection data, can be divided into a lower, high

reflectivity package (that likely contains magmatic elements) and an upper, transparent or less reflective sequence. The upper package forms a sag basin vertically aligned with the uplifted Moho, whereas the lower unit seems to be faulted, displaying sedimentary wedge geometries against faults (poor seismic quality). Considering wedge and crustal geometries, faults in the lower part of the sequence have been interpreted to dip dominantly landward and to branch at the transition between the upper and the lower-middle crust that is roughly identified in the seismic profile at a depth of ~20 km. Lower syn-rift units appear to be underlain by older, pre-rift sediments in this profile (the top basement likely represents the top pre-rift in Fig. 9). Younger Jurassic and Cretaceous sequences overlay the Louann Salt. They are folded and thicken progressively towards the uplifted Moho area.

In the distal rift, located in the deep Florida offshore (Fig. 10), the Moho shallows progressively southward to reach a minimum depth of ~ 11 km at the OCT. Extensional faults affecting the continental crust are well imaged to the north of the distal rift (Fig. 10). They have an intermediate dip, can be tracked up to a depth of 13-14 km and probably detach at the intra-crustal boundary between the upper, brittle and the middle-lower, ductile crust (decoupled domain, Fig. 10). Further South, basement faulting controlled the sedimentation of a pre-salt sequence that is poorly imaged in the central part of figure 10. Based on observed and inferred thickness variations, we divided it into an upper and a lower sequence (Fig. 10). The lower sequence seems to display syn-tectonic wedge geometries in the northern and central area of the profile (poor seismic quality) whereas to the South, both the upper and the lower sequences thin progressively basinward to finally pinch-out close to the continent-ocean boundary. These units pre-date faulting in the distalmost domain (i.e., they are offset by extensional basement faults and do not show sharp thickness variations across them) which suggests a progressive oceanward migration of faulting as also observed in the central Yucatan margin (Fig. 8). Fault migration is also supported by the geometrical relationship between the base Louann Salt and the extensional

basement faults: the base of salt is un-faulted to the North (i.e., post-faulting) but it is offset by faults in the distalmost rifted crust (i.e., pre- to syn-faulting).

The OCT is interpreted as a narrow exhumed mantle domain in North Florida (also identified by Pindell et al., 2014, 2016, 2021; Rowan, 2018) and a magmatic zone, involving extrusives and intrusives, in the central Yucatan margin (Fig. 8). The exhumed mantle domain in North Florida (Fig. 10) is partly overlain by a thin, faulted continental crust defining several basement highs and lows (Rowan, 2018). Faults in this domain affect the thinned continental crust and the upper part of the mantle and they are dominantly oceanward dipping, although a major continent-ward dipping structure is identified close to the distal limit of the continental crust (see LCC in Fig. 10). Faults in this domain offset the base of the Louann Salt and fold the top salt envelope, which likely indicates that fault activity in the North Florida OCT continued after salt deposition. Nevertheless, the base salt remains un-faulted across the OCT in the central Yucatan section, where it drops smoothly into a wide outer trough (Rowan, 2018; Hudec and Norton, 2019; Steier and Mann, 2019). The top of the oceanic crust is located at an average depth of ~ 11 km whereas the oceanic Moho is imaged at 16-18 km, being slightly shallower in the central Yucatan margin than in the North Florida margin. The thickness of the oceanic crust is 6-8 km.

Mobile salt extends across the deepest offshore in the central Yucatan and North Florida domains and the Florida platform. The distal salt pinch-out is located at the OCT, evidencing that salt deposition was completed before oceanic spreading in the central cross-section (as also suggested by previous authors, Pindell, 1985; Bird et al., 2005; Hudec et al., 2013; Pindell et al., 2018). Gravity gliding of supra-salt units has been largely recognized and described in the cross-section area (Fig. 8, 9; Horn et al., 2017; Hudec and Norton, 2019; Steier and Mann, 2019; Pilcher et al. 2014; Rives et al., 2019; Miranda-Madrigal et al., 2021). This gliding was probably easier in the central Yucatan domain, where the base salt remains largely un-faulted at the distal continental crust and the OCT but it was likely hampered by basement faults deforming the base and top salt in the North Florida OCT.

3.3.3. The western cross-section: West Yucatan-offshore Texas

The West Yucatan cross-section (Fig. 11) is subperpendicular (slightly oblique) to the LOC and to early rift structures. As previously introduced, it is based on seismic reflection data in the Yucatan margin and was roughly completed to the North using the seismic refraction profile Gumbo-2 (see location in Fig. 1, Van Avendonk et al., 2015; Eddy et al., 2018;). The velocity model across this refraction profile suggests that the continental Moho is located at a maximum depth of ~26 km in its northern boundary whereas the top basement is modelled at depths of 12-15 km (Eddy et al., 2018). Maximum crustal thicknesses ranging between 11 and 14 km are thus estimated along a minimum extent of ~200 km which indicates that the extended crust in this area is wider than this value.

>30 km-thick crust is preserved in the southernmost part of the West Yucatan margin (Figs. 11, 12), where the Moho is imaged at an approximate constant depth of ~ 36 km and the top basement is found at ~ 5 km depth. Rifting concentrates along a ~200 km-wide zone where crustal thickness decreases progressively up to a minimum of 1-2 km at the OCT. The Moho shows a stepped geometry defined by two southward dipping segments (Fig. 11) that bound an intermediate ~ 100 km-wide domain where the Moho is roughly flat. The top basement remains flat and un-faulted in the Yucatan platform but is faulted in the deepest Yucatan offshore where top basement depth increases. Pre-salt units in this area (Fig. 12) have similar thicknesses to those observed in the central Yucatan cross-section. They include a lower, high reflective package, probably involving magmatic units (labelled as 'older package' in Fig. 12), and an upper, less reflective sequence likely made of sedimentary units (including the 'intermediate and younger packages' in Fig. 12).

Basement faults in the rifted crust are dominantly landward dipping, although a major oceanward dipping structure is observable at the transition between the distal rift and the OCT. The relative time-relationship between faulting and sedimentary units in the syn-rift sequence indicates a basinward

migration of rifting: in the rifted continental crust, basement faults are coeval to the sedimentation of the oldest syn-rift units (older and intermediate-age sequences in Fig. 12) whereas faulting at the OCT post-dates the sedimentation of the youngest pre-salt units ('younger sequence', showing a sag-type distribution over the previous syn-tectonic sequence). Overlying these units, the base of the Louann Salt dips shallowly to the North and remains largely un-faulted except in the distalmost continental crust and the OCT.

In the OCT, crustal thicknesses are almost zero, and pre-salt sedimentary units are highly intruded. This defines a narrow, exhumed mantle domain with magmatic contribution that was not recognized across the central nor the eastern Yucatan cross-sections. The Louann Salt drops down in the OCT area where it defines a narrow outer trough bounded landward by the previously mentioned, major and oceanward dipping fault. Salt in this outer trough is limited, partly disrupted by faults and overlain by post-salt, Jurassic sedimentary units forming a small, syn-exhumation depocenter (see label in Fig. 12). The configuration of pre-, syn- and post-salt units at the OCT indicates that magmatic accretion, mantle exhumation and faulting in this area occurred partly after salt deposition (i.e., salt pinches-out landwards of the LOC and certain faults offset the salt and post-salt units that overlay magmatic additions).

The Late Jurassic and Cretaceous units are thinner than in the central Yucatan cross-section, although Cenozoic units are conversely thicker. Salt tectonics in the West Yucatan cross-section is very limited (Hudec and Norton, 2019, Figs. 8 and 12). The oceanic crust is well imaged in the western Yucatan cross-section, where it shows a 5-6 km thickness. Conversely, in the southern boundary of the Gumbo-2 profile (Texas offshore, Fig. 11), the modelled oceanic crust is thicker (8.5-9 km), the oceanic Moho being interpreted at a depth of 20 km (Eddy et al., 2018).

3.3.4. Summary and comparison between the three crustal-scale cross-sections. Comparison to previous interpretations.

The comparison between the three interpreted cross-sections (Figs. 4 to 12) shows significant along-strike variations in the geometry of the Gulf of Mexico conjugate margins. Regarding crustal geometries, cross-sections are characterized by (i) a proximal zone where the crust is ≥ 30 km-thick and (ii) a distal zone where rifting concentrates and the crust tappers oceanward. In the first zone, Moho depths (~ 36 to 40 km) and crustal thicknesses (~ 31 to 34 km) are similar in the three cross-sections. The second zone defines a ~100-150 km-wide domain in the South-Florida-East Yucatan line, but this domain is wider (~200-250 km) in the North Florida-Central Yucatan and West-Yucatan profiles. In terms of syn-rift and OCT geometries, strong similarities are found between the latter (North Florida-Central Yucatan and West-Yucatan cross-sections). They show thick syn-rift depocenters underneath the Louann Salt that are characterized by syn-tectonic wedge and sag geometries and contain high reflectivity packages. The strong reflections suggest the presence of magmatic elements and are observed in the lower units of the Apalachicola basin and the lower portion of the decoupled domain in the Central and West Yucatan cross-sections. They grade into less reflective or semi-transparent units of probable sedimentary nature that are dominant in the distal part of the rifted crust and the uppermost pre-salt. Over them, the base of the Louann Salt is un-faulted except in the distalmost continental crust and the OCT. Salt is mobile and relates to a gravity gliding system that is better developed in the central cross-section but limited in the western one. Finally, the OCT in the North Florida-Central Yucatan and West-Yucatan profiles corresponds to a narrow (<15-20 km-wide) exhumed mantle and/or magmatic domain that predates lithospheric break-up and formation of stable oceanic crust. Significant differences are observed between these two cross-sections (North Florida-Central Yucatan and West-Yucatan) and the South Florida-East Yucatan profile where: (i) pre-salt units are absent or very thin, (ii) the Louann evaporites are part of the syn-rift sequence, they are fault-bounded and show reduced to no salt mobility and (iii)

the transition between the continental and the oceanic crust is sharp (no exhumed mantle or magmatic, transitional zone has been identified).

In the West Florida margin, additional constraints on crustal geometries derive from the two seismic refraction profiles extending along the margin (see location of Gumbo-3 and Gumbo-4 in Fig. 1a). Comparison between these refraction lines (Christeson et al., 2014; Eddy et al., 2014) and the South and North Florida cross-sections (Fig. 4, 6, 9, 10) shows a number of similarities and differences. In the proximal part, Moho depths determined from seismic refraction (~ 32-33 km in Gumbo-4 and ~ 34 km along Gumbo-3, Christeson et al., 2014; Eddy et al., 2014) are similar although slightly shallower than those defined in the seismic reflection profiles (~ 36 km in the South Florida cross-section and up to ~ 40 km in the easternmost portion of the North Florida cross-section). Note that the seismic refraction profile Gumbo-4 is at an average distance of ~ 250 km from the seismic reflection line considered in this study and traverses an early rift basin where the continental crust is expected to be thinner (Fig. 1a). Crustal wedge geometries and Moho depths in the deep offshore are similar in both seismic refraction and reflection profiles although the mantle exhumation domain in North Florida, defined in this and previous studies (Pindell et al., 2014; Rowan, 2018), is not considered in the model derived from the Gumbo-3 section (Eddy et al., 2014). In the latter, seismic velocities along the Apalachicola basin are too high (5.0–6.5 km/s) for an entirely sediment-filled basin, and are interpreted to represent basalts and volcanoclastic sediments (Eddy et al., 2014). The Apalachicola rift overlaps a NW-SE-trending gravity high and magnetic anomaly that disappears laterally to the East (see location of 'gravity high' in Fig. 1a). The strongly reflective, south-dipping reflections at the base of the basin (Fig. 9) involve a dense, highly magnetic material of magmatic origin (Liu et al., 2019), as interpreted in this and previous studies. Similarly, these high reflective units have been also identified in the deep offshore along seismic reflection profiles to the south of the North Florida cross-section in this work (Imbert and Philippe, 2005; Pindell et al., 2014; Curry et al., 2018). They have been interpreted either as magmatic SDRs (Imbert and

Philippe, 2005) or as igneous inputs via diking or volcanics interbedded within sedimentary units (Pindell et al., 2014; Curry et al., 2018). This second option is in agreement with our interpretation of the Apalachicola basin and the earliest syn-rift units in the Central and West Yucatan cross-sections.

Underlying the Apalachicola basin, the shallowing Moho interpreted from seismic reflection profiles (Fig. 9) corresponds to a zone of anomalously high velocities (in this area, the 7.5 km/s contour line shallows up to a minimum depth of ~27 km). The interpreted Moho uplift is consistent with gravity and magnetic data (Liu et al, 2019). Conversely, based on refraction data, Eddy et al (2014) propose either syn-rift magmatic underplating near the Moho, or syn-rift intrusions into the lower continental crust to explain high seismic velocities. Underplating and/or magmatic additions into the lower crust in this area cannot be discarded and its potential influence on crustal area and crustal extension calculations is considered in section 4.2. from this study. Similarly, intrusive bodies at the base of the crust are also interpreted in gravity and magnetic modelling studies along the central and western Yucatan areas (Filina and Hartford, 2021).

4. Crustal extension and crustal domains: along dip organization and along strike variations

4.1. Definition of crustal domains

Crustal domains and their lateral variation throughout the study area can be defined by analyzing the shape of the crust across the three cross-sections described in section 3.3 (Fig. 13). The interpreted crust is bounded by two main surfaces, the Moho and the top basement. In addition, the base of the post-rift sequence has also been considered, approximated by the base of the Louann Salt in the central and western cross-sections. Based on the geometry of the Moho, the continental crust has been divided into four different domains (Chauvet et al., 2020): the proximal domain, the proximal necking, the thinned domain and the distal necking. In the central and western cross-sections, a fifth domain is identified at

the ocean-continent transition (OCT in Fig. 13). These crustal domains are delimited by more or less prominent inflexions of the Moho surface (i.e., Moho hinge lines in Chauvet et al., 2020), rely on the depth-migration and depth-conversion of the seismic data and assume the inherent uncertainty related to depth processing (preSDM in the considered seismic lines).

The proximal domain in the interpreted cross-sections (Fig. 13) is characterized by Moho and top basement horizons that are approximately parallel and flat (e.g., Péron-Pinvidic et al., 2017; Chauvet et al., 2020), except for some minor normal faulting offsetting the basement in the East Yucatan margin. They bound a ≥ 30 km-thick crust that is no or weakly thinned. The basement is overlain by a syn-rift sequence (i.e., sequence comprised between the top basement/top pre-rift and the base post-rift/base salt) that is very thin or absent and a post-rift sequence (i.e., sequence comprised between the base post-rift/base salt and the sea-bed) that thickens westward (Fig. 13). The proximal necking is characterized by a convergence of the Moho and the top basement (Chauvet et al., 2020). It is separated from the proximal domain by the Proximal Moho Hinge Line (PHL1 in Fig. 13) whose position is defined at the locus of the first Moho inflection (which is not necessarily corresponding to the first top basement inflection, Fig. 13). Across the considered profiles, the proximal necking widens from the South Florida-East Yucatan cross-section (40-55 km) to the West, being shorter in the Mexico margin (40-75 km) and larger in the United States margin (55-210 km, Fig. 13). Moho slopes across the proximal necking are shallow (Fig. 13) and the geometry of the top basement changes laterally: it describes a rough synformal geometry in the South and North Florida margins but it is flat in the West and East Yucatan margins or flat and then basinward dipping in the central Yucatan cross-section. In the three profiles across Yucatan, the top basement shows an inflection that is shifted oceanward with regard to the Moho inflection, which could indicate areas where the upper crust remains undeformed but the middle-lower crust thins by ductile flow.

Oceanward of the proximal necking, the thinned domain is defined by a distal continental crust wedge characterized by crustal thicknesses below ~15 km and a Moho surface that dips generally less than in the proximal necking. This domain is separated from the proximal necking by a second Moho inflection (Proximal Moho Hinge Line 2, PHL2 in Fig. 13) and broadens progressively westward in both the Mexico and the United States margins. It is separated from the distal necking by a third Moho inflection (Distal Moho Hinge Line, DHL in Fig. 13) that is located at distance of 10-15 km from the LCC in the central and western cross-sections and of 30-45 km in the eastern one. The Moho in the distal necking is generally steeper than in the thinned domain and the proximal necking. Oceanward of the distal necking, a ~15-20 km-wide OCT domain (exhumed mantle, magmatic additions and small-scale continental crust bodies) is identified in the central Yucatan, West Yucatan and North Florida cross-sections (Fig. 8, 10, 12).

The crustal domains identified in Figure 13 (following the approach of Chauvet et al., 2020) are comparable and similar to crustal domains amply defined in previous margin studies (e.g. Péron-Pinvidic and Manatschal, 2009; Mohn et al., 2012; Péron-Pinvidic et al., 2013; Sutra et al., 2013; Tugend et al., 2015; Sapin et al., 2021): the distal necking approximately corresponds to the coupled domain (Sutra et al., 2013) whereas the proximal necking and thinned domains considered together are roughly equivalent to the necking domain (Mohn et al., 2012; Péron-Pinvidic et al., 2013, 2017). The outer limit of the necking domain would overlap the PHL1, except in the North Florida cross-section, where the aborted rift could be considered as part of the proximal domain (similarly to the Galicia Interior Basin in the Iberian margin, Péron-Pinvidic et al., 2013).

4.2. Calculation of horizontal extension values

Bulk extension across the presented cross-sections is estimated using the area balancing method (Gibbs, 1983; Pindell, 1985; Rowan and Kligfield, 1989; Pindell et al., 2021). This method is based on the calculation of the area of the continental crust in present-day coordinates (i.e., area of the polygon

bounded by the top basement and the continental Moho) and its restoration to pre-rift stages, assuming it had a constant thickness across the area where the rifted margin developed and that deformation is restricted to the cross-section plane (i.e., plain strain hypothesis). The comparison between the length of the present-day rifted margin and the pre-rift template obtained after area restoration allows estimating the amount of horizontal extension that was accommodated during continental rifting stages (similarly to Sutra et al., 2013; Fig. 14).

Area restorations are purely geometric and independent of the mechanisms producing crustal extension. They consider two main assumptions: (1) the area of the continental crust remained constant across the cross-section plane (no area gains nor area losses through time) and (2) the crustal thicknesses observed in the non-rifted zone are representative of crustal thicknesses before rifting. Crustal areas were calculated using the software Move (Petroleum Experts) and two different approaches were applied: first, we considered the area of the whole continental crust and later on we considered and restored the areas of the upper and the lower-middle crust separately. This second approach allows to indirectly and very roughly estimate the partitioning between the brittle and ductile counterparts of the deformation. Both methods have inherent uncertainties that derive from different sources of error: (i) the inaccuracy in the picking of the Moho, the top basement and the upper/middle-lower crust boundary, (ii) the uncertainty in the depth processing of seismic lines that directly affects the estimation of crustal areas and thicknesses, (iii) the possibility of crustal area changes during the rifting process or later tectonic events (such as magmatic additions to the crust) and (iv) the potential obliquity between the extension direction during rifting and the direction of the available seismic reflection profiles. For the cross-sections considered in this study, the uncertainties related to (i) and (ii) are assumed to be relatively low because the horizons used for the area calculations are well-imaged in PreSDM processed seismic reflection profiles and mostly consistent with available seismic refraction data. The upper/ lower-middle crust boundary in the North Florida cross-section is an exception, and it

is not considered for extension calculations from upper and middle-lower crust areas separately (Fig. 14). Regarding the potential contribution of magmatic additions to the crust, we minimized their effect on the extension calculations: syn-rift magmatism at the OCT and certain parts of the decoupled rift was identified and discarded for crustal area calculations. Nevertheless, area estimates in the North Florida, Central Yucatan and West Yucatan cross-sections could be impacted by the presence of magmatic additions into the lower continental crust (as interpreted along the seismic refraction profile Gumbo 3 and along gravity and magnetic profiles in the Yucatan margin; Eddy et al., 2014; Filina and Hartford, 2021). In addition, obliquity between rifts, regional extension direction and cross-section traces is a likely source of error in the Gulf of Mexico that results in an underestimation of crustal extension values. Our cross-sections are perpendicular to moderately oblique to late rift (phase-2) and early rift (phase-1) extensional faults, except in South Florida, where the considered seismic profile runs highly obliquely (~25º) to phase-1 structures. As mentioned before, this cross-section traverses a NE-trending basement high (the Tampa Arch, mapped in Fig. 1a from Pindell et al., 2014, 2021) where crustal thicknesses are ~ 32- 33 km (Fig. 4) and Triassic-Jurassic syn-rift sediments are absent or very thin (<250 m; Frederick et al., 2020). The relatively thick crust and the thin syn-rift along this basement high indicate that the extension during early rifting stages was probably negligible along the cross-section trace, the extension being thus mostly accommodated in late rift (phase-2) stages. Conversely to the eastern cross-section, our central and western profiles traverse early (Miranda-Peralta et al., 2014; Frederick et al., 2020; Storey, 2020; Pindell et al., 2021) and late rift basins, they both contributing to the crustal extension recorded along the cross-sections.

For the whole crust restorations (Table 1), pin-lines are located at the LCC (that overlaps with the LOC in the eastern cross-section, Fig. 14). Results (Fig. 14, Tables 1 and 2) show strong variations in continental extension values across and along the considered cross-sections. The United States portion of the cross-sections is more extended than the Mexico one: 70 versus 52 km and 140 versus 101 km in the eastern

and central cross-sections, respectively (see Table 1, values from the whole crust area). Besides, restorations (Table 1, 2, Fig. 14) indicate an increase in the total extension from the South Florida-East Yucatan to the North Florida-Central Yucatan cross-sections. When both, the Mexico and United States continental margins are considered, a total extension of 122 and 241 km can be estimated for the eastern and central cross-sections, respectively. This increase in extension values relates at a great extent to the fact that the eastern cross-section runs through a basement high where phase-1 extension was minimal whereas the central cross-section traverses both phase-1 and phase-2 basins (Fig. 1a). Cross-section traces in West Yucatan and North Florida are moderately oblique to these early and late rifts, and calculated extension values are thus probably underestimated (i.e., the obtained 110 and 140 km should be considered as a minimum crustal extension value). In the North Florida cross-section, the potential error related to an underestimated volume of magmatic additions in the lower crust was evaluated. Along the refraction profile Gumbo 3 (Eddy et al., 2014), the highly intruded, lower crust bodies represent ~ 14% of the area of the whole crust. Taking into account this percentage, and assuming that magmatic additions in the intruded lower crust bodies could represent a 50 to 80% of their area, an underestimation of ~13-16 km in the crustal extension calculated for the North Florida cross-section should be considered. This result indicates that the existence of magmatic intrusions in the lower crust (not defined from the seismic reflection profiles in this study) may lead to underestimations in crustal extension values that are probably < 20 km.

Slight differences are observed when restorations are done for the whole crust or for the upper and middle/lower crust separately (see restored polygons in Fig. 14). Nevertheless, misfits in the pre-rift crustal lengths are less than 10 km (Fig. 14) which indicates that upper and lower/middle crust deformations are approximately balanced.

Cross-section	Margin	Crustal thickness in the proximal	Area of the whole crust	Present-day length of the margin (km)	Length of the margin in pre-rift stages (km)	Amount of extension (km)

		margin (km)	(km^2)			
Eastern cross-section	South Florida	33	8701	335	265	**70**
	East Yucatan	32.5	5657	226	174	**52**
Central cross-section	North Florida	34	5900	314	173.5	**140.5**
	Central Yucatan	31.5	6045	293	192	**101**
Western cross-section	West Yucatan	31	5844	299	188.5	**110.5**

Table 1. Area restorations using the whole crust. Extension values in kilometers are indicated in the last column.

Cross-section	Margin	Upper crust thickness, proximal margin (km)	Lower crust thickness, proximal margin (km)	Area upper crust (km^2)	Area middle-lower crust (km^2)	Length upper crust in pre-rift stages (km)	Length middle-lower crust in pre-rift stages (km)	Difference between the lengths of the upper and the whole crust in pre-rift stages (km)	Difference between the lengths of the middle/lower and the whole crust in pre-rift stages (km)
Eastern cross-section	South Florida	11	22	2932	5769	266.5	256.5	1.5	-8.5
	East Yucatan	11	21.5	1900	3757	173	175	-1	1
Central cross-section	Central Yucatan	10.5	21	1961	4084	187	194.5	-5	2.5
Western cross-section	West Yucatan	11	20	2122	3722	193	186	4.5	-2.5

Table 2. Area restorations considering the upper and the middle/lower crust separately. See graphical results of the restoration in Figure 14.

4.3. Along-strike variation in crustal domains and correlation with the distribution of salt and pre-salt units

The crustal domains identified in the cross-sections of the Gulf of Mexico conjugate margin (Fig. 13) have been laterally correlated and westward expanded using previous interpretations (Hudec et al., 2013; Minguez et al., 2020) and additional seismic refraction (Christeson et al., 2014; Van Avendonk et al., 2015; Eddy et al., 2014, 2018), gravity (Bonvalot et al., 2012; Sandwell et al., 2014) and magnetic anomalies data (Maus et al., 2009) to build the structural domains maps in Fig. 15 and in the Supplementary Material. The maps illustrate the regional-scale distribution of crustal domains and their relationship to the extent of the Louann Evaporites (Fig. 15a) and the underlying pre-salt units (Fig. 15b). This areal relationship is based on the observations done in the cross-sections (Figs. 4 to 12), from which the crustal and sedimentary thicknesses correlation graphics in Fig. 16 were also derived.

Continental crust domains run roughly parallel to gravity anomalies in the Yucatan and Florida margin rifted crust (see Bouguer anomaly in Fig. 15a and vertical gravity gradient derived from satellite altimetry in the Supplementary Material). In the Mexico margin, a progressive, oceanward increase in the Bouguer gravity anomaly (Bonvalot et al., 2012) occurs across the distal part of the proximal necking, the thinned domain and the distal necking (Fig. 15a), accordingly with the progressive thinning of the continental crust in this area (Fig. 16). Maximum Bouguer gravity anomalies are found at the OCT and the LOC. In the United States margin, the pattern of gravity lows and gravity highs becomes more complex (Fig. 15a). Along the North Florida cross-section, they run approximately parallel to the LOC (curving from NW-SE in the East to NE-SW in the West), and are discontinuous, showing frequent lateral terminations and along-strike relays. Further to the South (Central and South West Florida), gravity highs are perpendicular and parallel to the LOC, likely depicting the interference between phase-1 and phase-2 structures. A good correlation is observed between the proximal rift in the North Florida cross-section (Apalachicola basin, Fig. 9) and a NW-SE-trending gravity high (see location in Fig. 15a). This gravity high

continues laterally to the West which likely indicates that the rifted zone extends in this direction, underneath the allochthonous salt in the Sigsbee canopy. The northern margin of the gravity high approximately lies at the northern limit of seismic refraction profiles G1 and G2 (see location in Fig. 15a) where continental crustal thicknesses of 11 to 14 km have been interpreted (Van Avendonk et al., 2015; Eddy et al., 2018). These crustal thicknesses are in the range of those defined at the transition between the proximal necking and the thinned domain (see crustal thickness at PHL2 in Fig. 16), which led us to extend this crustal boundary at the northern limit of the mentioned gravity anomaly (Fig. 15a). Similarly, and as observed in the North Florida cross-section, the locus of PHL1 in the north-central and north-western Gulf of Mexico was tentatively defined at the northern limit of a positive Bouguer anomaly identified in onshore Louisiana and Texas (Fig. 15a), running parallel to the boundaries of the Texas-Arkansas-Louisiana Basin (TALB in Fig. 15b). To the East, we extended this crustal boundary as parallel to the South Georgia Basin (see mapping of phase-1 -rifts in Fig. 15b). The interpreted PHL1 roughly coincides with previous regional interpretations (Pascoe et al., 2016) and bounds a rifted continental crust that is considerably wider in the United States margin, where its plan-view geometry is marked by the interference between early and late rift structures (Fig. 15a). In the Yucatan margin (area constrained by the seismic-based cross-sections in this study), the rifted continental crust is narrower (< 280 km) and broadens from East to West. This confers the Gulf of Mexico a regional, across-strike asymmetry and along-strike non-cylindrical geometry.

The comparison between the proposed mapping of crustal domains and the map-view extent of the Louann Evaporites (modified from Rowan, 2014 and Snedden and Galloway, 2019, Fig. 15a) shows a direct correlation between the widths of the extended crust and the salt. The Louann Salt widens to the West, including anhydrite and mixed anhydrite and halite layers in the proximal areas of the eastern Gulf of Mexico (Snedden et al., 2018; Snedden and Galloway, 2019, Fig. 15a). Excluding the South Georgia Basin, the proximal pinch-out of the evaporites approximately overlaps PHL1 or is continent- or oceanward shifted by less than ~100 km with respect to this crustal boundary. The extent of the

evaporites in the Central and Western Yucatan and North Florida cross-sections (Figs. 8, 10 and 12) is slightly wider than the extent of the underlying pre-salt, syn-rift units (Figs. 15b). In the Mexico margin, pre-salt units concentrate along the distal part of the proximal necking, the thinned domain and the distal necking, being absent or very thin in the proximal domain and the OCT (Fig. 13, Fig. 16b, c). In the North Florida cross-section, the pre-salt extends along the proximal necking, the thinned domain and the distal necking (Fig. 15, 16). To the West of the cross-sections area, the N-S-trending Campeche magnetic anomaly and the NE-SW-trending Houston magnetic anomaly (see location in Fig. 15b) are in previous studies interpreted as the lateral continuation of the early syn-rift magmatism (intrusives and/or extrusives) in the north-central and western Gulf of Mexico (Mickus et al., 2009; Messager et al., 2019; Filina and Hartford, 2021). These units end laterally to the east (they are not identified in the South Florida cross-section, Fig. 4, 6). To the North of the Houston magnetic anomaly, sedimentation over the northern proximal necking is represented by the early rift sedimentary units of the Texas-Arkansas-Louisiana Basin (Fig. 2 and 15b; Salvador, 1987, 1991; Milliken, 1988; Snedden and Galloway, 2019; Wood and Benson, 2000) that in this area have sedimentary thicknesses of less than 2 km (Frederick et al., 2020).

As defined from gravity data, crustal domain boundaries approximately parallel magnetic anomalies (see total magnetic intensity in Fig. 15b and its vertical derivative in the Supplementary Material). These magnetic anomalies have been used to laterally extend the OCT domain identified in North Florida (Fig. 10), whose northern boundary is interpreted to follow a sequence of small wavelength anomalies (SWA in Fig. 15b; "en-echelon anomaly" in Minguez et al., 2020). The considered boundary is not clear from gravity anomalies (the gravity signal is highly influenced by the presence of thick salt in the north-central Gulf of Mexico), but it is consistent with previous interpretations (similar mapping proposed by Pindell et al., 2016; Minguez et al., 2020) and agrees with the 40-50 km wide exhumed mantle domain interpreted along the Gumbo 1 seismic refraction profile (van Avendonk et al., 2015). Location of the LOC in this area was taken from Hudec et al. (2013). Based on seismic data, they proposed that the limit

of the normal oceanic crust coincides with a landward-dipping basement ramp near the seaward end of the salt basin. If this boundary and our LCC are considered, the OCT domain in the United States margin would reach a maximum width in the central part and narrow progressively both to the West and to the East (Fig. 4). A similar along-strike width variation is identified in the Mexico margin where the OCT is nevertheless narrower than in the North. This interpretation disagrees with the previous structural domains map by Pascoe et al. (2016) that identifies a volcanic OCT all along the United States margin but limited to the eastern fragment of the Mexico margin.

5. Evolution of the Gulf of Mexico and comparison to other margins

5.1. Evolutionary model for the Gulf of Mexico during continental extension and OCT formation stages

From the cross-sections in this study, an evolutionary model can be proposed for the West Florida-Yucatan conjugate margin. Significant differences are inferred for the evolution of the North Florida, central and West Yucatan segments and the South Florida-East Yucatan profile.

5.1.1. Central and West Yucatan and North Florida cross-sections

The pre-salt, syn-rift units interpreted across the Central and West Yucatan and North Florida cross-sections (Figs. 8, 9, 10, 12) are (i) older than the overlying Louann Salt (Bajocian-Callovian; Olson et al., 2015; Pindell et al., 2019; Pulham et al. 2019, Snedden et al., 2019; Snedden and Galloway, 2019) and (ii) coeval to or younger than the detrital Eagle Mills unit (Triassic, Fig. 2; Salvador, 1987, 1991; Milliken, 1988; Snedden and Galloway, 2019; Wood and Benson, 2000; Frederick et al., 2020). Taking these age constraints into account, an Early to Middle Jurassic age can be considered for the sedimentary package underlying the salt whereas a Late Triassic to Early Jurassic age can be attributed to the older units containing magmatic elements in the lower syn-rift. This lower syn-rift package would be coeval to lava flows and igneous activity in the South Florida province (Heatherington and Mueller, 2003; Mickus et al.

2009; Fig. 2) and to magmatism in the Central Atlantic Magmatic Province (CAMP, ~200 Ma, Withjack et al., 1998; Marzoli et al., 2011) and Chiapas (Godinez-Urban, 2011a, b).

Considering the interpreted nature, age, distribution and faulting pattern of the pre-salt and salt packages in the central and western cross-sections in this study (Figs. 7 to 12), a three-stage evolutionary model can be proposed for this part of the Gulf of Mexico (schematically depicted in Fig. 17a).

In a first rifting stage, Late Triassic to Early Jurassic in age, seismic reflection (Pindell et al., 2014; Curry et al., 2018), seismic refraction (Eddy et al., 2014) and magnetic and gravity data (Liu et al., 2019; Filina and Hartford, 2021) suggest that magmatic elements were abundant within syn-rift units. These units (syn-rift involving magmatic elements in Fig. 17a) formed in different depocenters (diffuse rifting) encompassing high reflectivity packages that thickened towards the future break-up zone. Units forming these sequences are characterized by syn-tectonic wedge geometries, controlled by dominantly landward-dipping faults that likely detached on the upper- middle/lower crust transition (Figs. 8, 9 and 12). Syn-rift magmatism in the upper crust was probably accompanied by magmatic underplating near the Moho or syn-rift intrusions into the lower continental crust (Eddy et al., 2014; Filina and Hartford, 2021).

In a second rifting stage (Early to Middle Jurassic in age, Fig. 17a.2), magmatic activity probably decreased regionally, focalizing eastward in the Florida/Bahamas/Demerara/Guinea area where hotspot magmatism has been identified (Klitgord et al., 1984; Reuber et al., 2016; Basile et al., 2020; Museur et al., 2021). Syn-rift units in the Gulf of Mexico were mostly sedimentary. Sag sequences formed in the previously extended areas, whereas fault-related depocenters migrated towards the future break-up zone, as described from the configuration of pre-salt units in the western and central cross-sections in this study (Figs. 8, 10, 12). Seismic data point out that syn-rift sedimentation localized in a wide but unique depocenter controlled by basement faults that frequently cross-cut the whole crust.

Sedimentary wedges developed in the hangingwall of these faults and were subsequently overlain by a late, pre-salt sag sequence (as defined in the North Florida cross-section, Fig. 10, Rowan, 2018). During Early – Mid Jurassic times, the area of the central and western cross-sections evolved to a magma-poor rifting that localized over or close to the future break-up zone (Fig. 17a.2; also noted by Pindell et al. 2014, 2016, 2021; Rowan 2018).

Continued extension (Bajocian to Callovian, Fig. 17a.3) culminated with the exhumation of the mantle (Pindell et al., 2014; Rowan, 2018; Minguez et al., 2020) and/or the development of a magmatic OCT (as recognized in the central and western cross-sections in this study, Figs. 7 to 12). For the conjugate North Florida-central Yucatan margin, mantle exhumation and magmatism at the OCT occurred after a minimum continental crust extension of ~240 km. The relationship between salt and post-salt units and the different elements at the distal continental crust and the OCT (basement faults, magmatic additions and mantle exhumation surfaces) indicates that salt deposition across the central and western cross-sections was likely coeval to late continental thinning and early exhumation stages and was completed before the final configuration of the OCT and seafloor spreading (Pindell, 1985; Bird et al., 2005; Hudec et al., 2013; Pindell et al., 2018). The Louann Salt reached maximum, original thicknesses of 2-4 km along the northern Gulf of Mexico (Hudec et al., 2013) that were probably, considerably thinner across the studied profiles. Over the areas where Early to Mid-Jurassic rifting took place, salt was deposited forming a sag sequence (i.e., the base salt is largely un-faulted) and its thickness probably varied depending on the amount of previous crustal thinning.

5.1.2. South Florida - East Yucatan cross-section

The evolution depicted along the South Florida-East Yucatan cross-section (Fig. 17b) differs significantly from that of the central and western cross-sections (Fig. 17a). At crustal-scale, the rifted continental crust is narrower and the transition between the continental and oceanic crusts is sharper (no magmatic OCT nor exhumed mantle domain). Besides, in the South Florida-East Yucatan domain, (i) the syn-rift

units involving magmatic elements (Fig. 17a) seem to be absent, (ii) the Louann Evaporites or their lateral equivalent are coeval to continental rifting and include a mixture of halite and anhydrite facies (Snedden and Galloway, 2019), and (iii) they are overlain by an also syn-rift sedimentary package of Oxfordian age (Snedden and Galloway, 2019). The potential absence of Early Jurassic magmatism and the syn-rift nature of the Louann Salt equivalent indicates that continental rifting in the South Florida-East Yucatan area initiated later than in the central and western cross-sections zone. The onset of rifting took most probably place during Bajocian-Callovian stages (the Louann Salt equivalent is located at the base of the syn-rift package), coevally to mantle exhumation stages in the North Florida and central-western Yucatan domains. In this scenario, the pre-oceanic spreading evolution along the South Florida-East Yucatan cross-section can be summarized in the two main stages depicted in Figure 17b.

In a first rifting stage (Bajocian to Callovian in age, Fig. 17b.3), evaporites were deposited in a continental rift that, being centered at the future break-up zone, expanded across both the Mexico and Florida margins. Faults controlling salt deposition were doubly verging and probably detached in the upper- middle/lower crust transition. The accommodation space for evaporite deposition in the South Florida-East Yucatan domain was therefore created by brittle faulting of the upper crust (thermal and loading subsidence acted coevally in the area of the central and western cross-sections) which controlled the deposition of evaporites in small, fault bounded basins. The segmentation of salt bodies by faults (together with the presence of non-mobile anhydrite; Snedden et al., 2018; Snedden and Galloway, 2019) prevented gravity-gliding processes, that are absent in the eastern cross-section area.

In a second rifting stage (Oxfordian in age, Fig. 17b.4), fault activity and continental crust extension continued over the area occupied by the early rift and later syn-rift sediments covered early evaporites. Syn-rift units reach maximum thicknesses of 2-4 km in the East Yucatan-South Florida cross-section (Fig. 16), being much thinner than the pre-salt units identified in the central and western Yucatan cross-sections (7-8 km, Fig. 14). Oceanic crust accretion in the South Florida-East Yucatan cross-section area

occurred after a minimum continental crust extension of ~120 km (note that early, phase-1 rifting was highly oblique to the cross-section and negligible along the basement high it traverses).

5.2. Comparison to other margins

Although rifting in the Gulf of Mexico involved magmatism during the early syn-rift stages (coevally to the formation of the magma-rich margins of South Florida-Guinea-Demerara; Reuber et al., 2016; Museur et al., 2021), the margin was mostly magma-poor during the late syn-rift and break-up stages (Curry et al., 2018; Rowan, 2018; Sapin et al., 2021). Continental break-up involved mantle exhumation and also magmatic additions along the North Florida and central-western Yucatan areas. This is compatible with data from other case studies that show that typically considered magma-poor margins can record important magmatism during syn-rift and continental break-up (Alves et al., 2020 and references therein).

Classically considered magma-poor margins such as the NW Iberia (e.g., Sutra and Manatschal, 2012), South Australia – East Antarctica (e.g., Espurt et al., 2012; McCarthy et al., 2020) or Somalia margins (Mortimer et al., 2020; Hassan et al., 2020; Sapin et al., 2021) involve mantle exhumation domains. In these margins, exhumed mantle has been validated by drilling (Iberia-Newfoundland, Boillot et al., 1987) or dredges (East Antarctica, McCarthy et al., 2020) or interpreted from seismic profiles and gravity modelling (Somalia, Mortimer et al., 2020; Sapin et al., 2021). Mantle exhumation domains are wide across them: (1) in the NW Iberia margin, the exhumed mantle extends over more than 150 km (Egan and Meredith, 2007; Sutra and Manatschal, 2012; Dean et al., 2000); (2) in the Great Australian Bight margin, the exhumation domain forms a band that ranges in width from nearly 30 km to more than 100 km (Espurt et al., 2009; 2012) being 50-100 km wide in the Antarctic margin (McCarthy et al., 2020) whereas (3) the Somalia margin shows an also broad domain of exhumed mantle (> 200 km; Mortimer et al., 2020). In the central-western Yucatan and the North-Eastern Gulf of Mexico margin, these domains are contrarily narrower (OCT is <15-20 km wide for the considered cross-sections, although it

may widen in the north-central Gulf of Mexico, Fig. 15). More similar OCT widths are interpreted in the South Gabon-Angola margin (Péron-Pinvidic et al., 2017; Epin et al., 2021; Sapin et al., 2021) where the exhumed mantle domain displays maximum widths of less than 50 km in offshore Angola (Péron-Pinvidic et al., 2017), narrowing northward to the South Gabon offshore area (~15 km, Epin et al., 2021). In this second zone, the exhumed mantle evolves oceanward to a 15 to 30 km-wide outer high domain that is dominated by both extrusive and intrusive magmatism (Epin et al., 2021; break-up volcanics in Fernández et al., 2020), the OCT geometries and widths being very similar to those recognized across the central and western cross-sections in this study (Figs. 7, 11). Besides, salt represents an important element in the configuration of the South Gabon margin (Rowan, 2018; Fernández et al., 2020; Legeay et al., 2020). In South Gabon, as in the central and western cross-sections from this study, the base salt is locally offset by basement faults in the distalmost extended crust and OCT domain and it is interpreted as coeval to mantle exhumation or break-up volcanics (Rowan, 2018; Fernández et al., 2020; Epin et al., 2021). Similarly, narrow and deep outer troughs (10-15 km wide and ~2 km deep) can also be identified in seismic reflection profiles from this margin (compare cross-sections in Epin et al., 2021 to cross-sections in this study).

Besides being a dominantly magma-poor margin, the Gulf of Mexico shows some features that indicate a weak mechanical behavior of the continental crust (Sapin et al., 2021). In the cross-sections in this study, (1) the extended continental crust describes a wide wedge geometry, with widths that range from 90 to 275 km and Moho envelopes that dip <16º and (2) the middle-lower crust seems to be affected by kilometric-scale shears (Fig. 5, 6, 12) that likely indicate it has been deformed in a ductile manner (Clerc et al., 2018). Continental crust wedge geometries are similar to those defined in other margins such as the Iberia-Newfoundland (Afilhado et al., 2008; Sutra et al., 2013), the Bight Basin–Terre Adélie (Espurt et al., 2012) and the Gabon (Clerc et al., 2018) margins. In the latter, ductile shears are accompanied by crustal boudinage and frequent continentward dipping faults (as observed in the Gulf of Mexico margin) and the ductile behavior of the lower crust is attributed to (i) the effect of an initially weak crust

inherited from the Panafrican orogeny or (ii) an elevated thermal gradient (blanketing effect of syn-rift sediments, Clerc et al., 2015; 2018; or rapid mantle rise, Huismans and Beaumont, 2011).

In the cross-sections in this work, crustal wedge widths increase from the eastern to the central and western profiles (Fig. 12) together with the calculated crustal extension (Table 1, 2): the continental crust break-up occurred after a minimum extension of ~120 km in the South Florida-East Yucatan cross-section and over 240 km in the central and western profiles (Table 1, 2). Crustal extension values in the central cross-section area lie in the range of those estimated across the NW Iberia-Newfoundland (225-250 km; Sutra et al., 2013) and Australian-Antarctic conjugate margins (~200 km if mantle exhumation is discarded; Espurt et al., 2012) but are smaller along the eastern cross-section (~120 km). This extension decrease largely results from the location of the considered profiles with respect to early (phase-1) extensional basins. As previously described, the central and western cross-sections recorded extension related to Late Triassic-Early Jurassic rifting whereas the eastern cross section traverses an area where this early extension was minimal. Continental rifting in the eastern profile occurred coevally to the rotation of the Yucatan plate around a pole located in West Cuba (Fig. 1, Pindell et al., 2021 and references therein) and was partly synchronous to mantle exhumation, OCT formation and probably early oceanic accretion further to the West (the extension related to these processes is not included in the values given in section 4.2). Besides, crustal wedge widths and extension values required for break-up can be impacted by different parameters, including: (i) the initial mechanical strength of the continental crust, with weaker rheology relating to wider crustal wedges (Huismans and Beaumont, 2008; Liao and Gerya, 2014; Brune et al., 2016) or (ii) the extension rates (Rey et al., 2009; Brune et al., 2014; Tetreault and Buiter, 2018). Lateral variations in these two parameters, together with the previously mentioned observations (differential record of Late Triassic-Early Jurassic rifting and along-strike diachronism in continental rifting and break-up), could be considered to explain the narrowing of the continental crust wedge and the decreasing crustal extension identified in the South Florida-East Yucatan area.

6. Conclusions

In this study, we present three seismic-based, crustal-scale cross-sections running through the Florida and Yucatan domains (the South Florida-East Yucatan, North Florida-Central Yucatan and West Yucatan cross-sections). Seismic data in this area images crustal and syn-rift geometries and their interpretation indicates significant along-strike variations in the conjugate margins. The North Florida and central-western Yucatan sections are characterized by a 185 to 255 km-wide crustal wedge, which is separated from the oceanic crust by a narrow magmatic OCT or exhumed mantle domain. Syn-rift units attain maximum thicknesses of 7-8 km and involve a lower package that includes magmatic elements and an upper, sedimentary sequence. They are bounded by doubly-verging extensional faults showing rift migration from the proximal (older) to the distal (younger) part of the margin. These units are overlain by the Mid-Jurassic salt that expands over the extended crust and the OCT domain. By contrast, the South Florida-East Yucatan cross-section is characterized by a narrower crustal wedge (110 to 135 km) that changes sharply to the oceanic crust. Syn-rift units are considerably thinner (2 to 4 km) and, based on well, seismic facies criteria, and seismic correlation, include Mid-Jurassic evaporites and overlying sediments (Snedden and Galloway, 2019, this study).

Using the continental Moho as reference, we identified five crustal domains (proximal domain, proximal necking, thinned domain, distal necking and OCT) and calculated continental, horizontal extension values across the three constructed cross-sections. Minimum crustal extension values range between ~120 km in the eastern cross-section to ~ 240 km in the central one. The observations done in the cross-sections have been extrapolated in map view using previous interpretations and additional geophysical information (seismic, gravity and magnetic data) to build a crustal domains map that expands beyond the cross-sections area. This map depicts a rifted margin that is considerably wider in the United States margin (where its plan-view geometry is marked by the interference between early and late rift structures) and narrower in the Yucatan margin (where it broadens from East to West).

The presented dataset, together with previously published seismic interpretation and potential field modelling studies, supports that the Gulf of Mexico evolved from an early rifting involving magmatism to a magma-poor and weak margin where faulting migrated towards the future break-up zone and towards the south-eastern part of the margin. Break-up stages involved mantle exhumation and related magmatism, with the development of OCT domains that show strong similarities to those observed in the south Gabon margin.

Acknowledgments

This paper is the result of a research project funded by TotalEnergies Houston. The authors thank ION who kindly authorized us to publish their seismic data and J.F. Salel, L. Jensen, C. Nielsen and P. Ball for their critical view and the fruitful discussions on the Gulf of Mexico regional tectonics and rifted margins. We also thank our reviewers, James Pindell, Mohamed Gouiza and an anonymous reviewer, the comments by Athanasia Vasileiou, and the section editor Tiago Alves, who carefully read and constructively helped us to improve the quality of this manuscript.

References

Afilhado, A., Matias, L., Shiobara, H., Hirn, A., Mendes-Victor, L., Shimamura, H. (2008). From unthinned continent to ocean: The deep structure of the West Iberia passive continental margin at 38 N. *Tectonophysics*, *458*(1-4), 9-50.

Alves, T., Fetter, M., Busby, C., Gontijo, R., Cunha, T. A., Mattos, N. H. (2020). A tectono-stratigraphic review of continental breakup on intraplate continental margins and its impact on resultant hydrocarbon systems. *Marine and Petroleum Geology*, *117*, 104341.

Amante, C., Eakins, B.W., 2009. ETOPO1: 1 arc-minute global relief model: procedures, data sources and analysis. NOAA Tech. Mem. NESDIS NGDC24, Boulder(Co).

Antobreh, A. A., Faleide, J. I., Tsikalas, F., & Planke, S. (2009). Rift–shear architecture and tectonic development of the Ghana margin deduced from multichannel seismic reflection and potential field data. *Marine and Petroleum Geology*, *26*(3), 345-368.

Bain, J., Kegel, J., O'Reilly, C. (2019). Crustal interpretation by gravity, magnetics, and seismic data over the Gulf of Mexico. *GeoGulf Transactions,* 69, 319–331.

Basile, C., Girault, I., Paquette, J. L., Agranier, A., Loncke, L., Heuret, A., Poetisi, E. (2020). The Jurassic magmatism of the Demerara Plateau (offshore French Guiana) as a remnant of the Sierra Leone hotspot during the Atlantic rifting. *Scientific reports*, 10, 1-12.

Bird, D. E., Burke, K., Hall, S. A., Casey, J. F. (2005). Gulf of Mexico tectonic history: Hotspot tracks, crustal boundaries, and early salt distribution. *AAPG bulletin*, 89, 311-328.

Boillot, G., Recq, M., Winterer, E. L., Meyer, A. W., Applegate, J., Baltuck, M., ... & Williamson, M. (1987). Tectonic denudation of the upper mantle along passive margins: a model based on drilling results (ODP leg 103, western Galicia margin, Spain). *Tectonophysics*, *132*(4), 335-342.

Bonvalot, S., Balmino, G., Briais, A., M. Kuhn, Peyrefitte, A., Vales N., Biancale, R., Gabalda, G., Reinquin, F., Sarrailh, M., (2012). World Gravity Map. Commission for the Geological Map of the World. Eds. BGI-CGMW-CNES-IRD, Paris

Brune, S., Heine, C., Pérez-Gussinyé, M., Sobolev, S.V. (2014). Rift migration explains continental margin asymmetry and crustal hyper-extension. *Nature Communications*, 5, 1-9.

Brune, S., Williams, S. E., Butterworth, N. P., Müller, R. D. (2016). Abrupt plate accelerations shape rifted continental margins. *Nature*, 536, 201-204.

Chauvet, F., Sapin, F., Geoffroy, L., Ringenbach, J. C., Ferry, J. N. (2020). Conjugate volcanic passive margins in the austral segment of the South Atlantic–Architecture and development. *Earth-Science Reviews*, 103461.

Christeson, G. L., Van Avendonk, H. J. A., Norton, I. O., Snedden, J. W., Eddy, D. R., Karner, G. D., Johnson, C. A. (2014). Deep crustal structure in the eastern Gulf of Mexico. *Journal of Geophysical Research: Solid Earth*, 119, 6782-6801.

Clerc, C., Jolivet, L., Ringenbach, J.C. (2015). Ductile extensional shear zones in the lower crust of a passive margin. *Earth Planetary Science Lett*ers, 431, 1–7. doi:10.1016/j.epsl.2015.08.038.

Clerc, C., Ringenbach, J.C., Jolivet, L. Ballard, J.F. (2018). Rifted margins: Ductile deformation, boudinage, continentward-dipping normal faults and the role of the weak lower crust. *Gondwana Research,* 53, 20–40. https://doi.org/10.1016/j.gr.2017.04.030.

Curry, M. A., Peel, F. J., Hudec, M. R., Norton, I. O. (2018). Extensional models for the development of passive-margin salt basins, with application to the Gulf of Mexico. *Basin Research*, 30, 1180-1199.

Dallmeyer, R. D. (1989). Contrasting accreted terranes in the southern Appalachian Orogen, basement beneath the Atlantic and Gulf Coastal Plains, and West African orogens. *Precambrian Research*, 42, 387-409.

Davison, I. (2020). Salt Tectonics in the Sureste Basin, SE Mexico: some implications for hydrocarbon exploration. *Geological Society, London, Special Publications*, 504, 147-165.

Dean, S. M., Minshull, T. A., Whitmarsh, R. B., Louden, K. E. (2000). Deep structure of the ocean-continent transition in the southern Iberia Abyssal Plain from seismic refraction profiles: The IAM-9 transect at 40 20' N. *Journal of Geophysical Research: Solid Earth*, 105(B3), 5859-5885.

Deighton, I. C., Winter, F., Chisari, D. (2017). Recent high-resolution seismic, magnetic and gravity data throws new light on the early development of the Gulf of Mexico. In *AAPG Annual Meeting Abstracts, Houston*.

Duretz, T., Petri, B., Mohn, G., Schmalholz, S.M., Schenker, F.L. Müntener, O. (2016). The importance of structural softening for the evolution and architecture of passive margins. *Scientific Reports,* 6, 1–7.

Eddy, D. R., Van Avendonk, H. J., Christeson, G. L., Norton, I. O., Karner, G. D., Johnson, C. A., Snedden, J. W. (2014). Deep crustal structure of the northeastern Gulf of Mexico: Implications for rift evolution and seafloor spreading. *Journal of Geophysical Research: Solid Earth*, 119, 6802-6822.

Eddy, M. P., Jagoutz, O., Ibañez-Mejia, M. (2017). Timing of initial seafloor spreading in the Newfoundland-Iberia rift. *Geology*, *45*(6), 527-530.

Eddy, D. R., Van Avendonk, H. J., Christeson, G. L., Norton, I. O. (2018). Structure and origin of the rifted margin of the northern Gulf of Mexico. *Geosphere*, 14, 1804-1817.

Egan, S. S., Meredith, D. J. (2007). A kinematic modelling approach to lithosphere deformation and basin formation: application to the Black Sea. *Geological Society, London, Special Publications*, 282, 173-198.

Epin, M. E., Manatschal, G., Sapin, F., Rowan, M. G. (2021). The tectono-magmatic and subsidence evolution during lithospheric breakup in a salt-rich rifted margin: insights from a 3D seismic survey from southern Gabon. *Marine and Petroleum Geology*, 128, 105005.

Espurt, N., Callot, J.P., Toterdell, J., Struckmeyer, H., Vially, R., (2009). Influence of continental breakup dynamics on large-scale delta system evolution. Insights from the Cretaceous Ceduna delta system, Bight basin, South Australian margin. *Tectonics*, 28, TC6002, doi:10.1029/2009TC002447.

Espurt, N., Callot, J.-P., Roure, F., Totterdell, J.M., Struckmeyer, H.I.M., Vially, R. (2012). Transition from symmetry to asymmetry during continental rifting: an example from the Bight Basin-Terre Adélie (Australian and Antarctic conjugate margins). *Terra Nova,* 24, 167-180. http://dx.doi.org/10.1111/j.1365-3121.2011.01055.x

Ewing, T. E., Galloway, W. E. (2019). Evolution of the Northern Gulf of Mexico Sedimentary Basin. In *The Sedimentary Basins of the United States and Canada* (pp. 627-694). Elsevier.

Faleide, J. I., Tsikalas, F., Breivik, A. J., Mjelde, R., Ritzmann, O., Engen, O., Wilson, J., Eldholm, O. (2008). Structure and evolution of the continental margin off Norway and the Barents Sea. *Episodes*, 31, 82-91.

Fan, C., Xia, S., Cao, J., Zhao, F., Sun, J., Wan, K., Xu, H. (2019). Lateral crustal variation and post-rift magmatism in the northeastern South China Sea determined by wide-angle seismic data. *Marine Geology*, *410*, 70-87.

Feng, J., Buffler, R. T., Kominz, M. A. (1994). Laramide orogenic influence on late Mesozoic-Cenozoic subsidence history, western deep Gulf of Mexico basin. *Geology*, *22*(4), 359-362.

Fernández, O., Olaiz, A., Cascone, L., Hernandez, P., Pereira, A. D. F., Tritlla, J., ... & Tur, N. (2020). Geophysical evidence for breakup volcanism in the Angola and Gabon passive margins. *Marine and Petroleum Geology*, *116*, 104330.

Filina, I., Hartford, L. (2021). Subsurface structures along western Yucatan from integrated geophysical analysis. *Marine and Petroleum Geology*, 104964.

Franke, D., Neben, S., Ladage, S., Schreckenberger, B., Hinz, K. (2007). Margin segmentation and volcano-tectonic architecture along the volcanic margin off Argentina/Uruguay, South Atlantic. *Marine Geology*, 244, 46-67.

Frederick, B. C., Blum, M. D., Snedden, J. W., Fillon, R. H. (2020). Early Mesozoic synrift Eagle Mills Formation and coeval siliciclastic sources, sinks, and sediment routing, northern Gulf of Mexico basin. *Geological Society of America Bulletin*, 132, 2631-2650.

Fredrich, J. T., Fossum, A. F., Hickman, R. J. (2007). Mineralogy of deepwater Gulf of Mexico salt formations and implications for constitutive behavior. *Journal of Petroleum Science and Engineering*, 57, 354-374.

Froitzheim, N., Manatschal, G. (1996). Kinematics of Jurassic rifting, mantle exhumation, and passive-margin formation in the Austroalpine and Penninic nappes (eastern Switzerland). *Geological society of America bulletin*, 108, 1120-1133.

Galloway, W. E. (2008). Depositional evolution of the Gulf of Mexico sedimentary basin. *Sedimentary basins of the world*, *5*, 505-549.

Galloway, W. E., Whiteaker, T. L., Ganey-Curry, P.E. (2011). History of Cenozoic North American drainage basin evolution, sediment yield, and accumulation in the Gulf of Mexico basin. *Geosphere*, 7, 938–973.

Geoffroy, L., Burov, E. B., Werner, P. (2015). Volcanic passive margins: another way to break up continents. *Scientific reports*, 5, 1-12.

Gernigon, L., Franke, D., Geoffroy, L., Schiffer, C., Foulger, G. R., Stoker, M. (2019). Crustal fragmentation, magmatism, and the diachronous opening of the Norwegian-Greenland Sea. *Earth-Science Reviews,* 102839. https://doi.org/10.1016/j.earscirev.2019.04.011

Gibbs, A. D. (1983). Balanced cross-section construction from seismic sections in areas of extensional tectonics. *Journal of structural geology*, 5, 153-160.

Godínez-Urban, A., Lawton, T.F., Molina-Garza, R.S., Iriondo, A., Weber, B., and López-Martínez, M., (2011a). The Jurassic volcanic and sedimentary rocks of La Silla and Todos Santos formations, Chiapas: Record of Nazas arc magmatism and rift basin formation prior to opening of the Gulf of Mexico: Geosphere, v. 7, p. 121–144, https://doi.org/10.1130/GES00599.1.;

Godínez-Urban, A., Molina-Garza, R.S., Geissman, J.W., and Wawrzyniec, T.F., (2011b). Paleomagnetism of the Todos Santos and La Silla Formations, Chiapas: Implications for the opening of the Gulf of Mexico: Geosphere, v. 7, p. 145–158, https://doi.org/10.1130/GES00604.1

Gouiza, M., Paton, D. A. (2019). The Role of Inherited Lithospheric Heterogeneities in Defining the Crustal Architecture of Rifted Margins and the Magmatic Budget During Continental Breakup. *Geochemistry, Geophysics, Geosystems*, *20*(4), 1836–1853. https://doi.org/10.1029/2018GC007808

Haq, B. U. (2014). Cretaceous eustasy revisited. *Global and Planetary Change*, 113, 44–58, doi:10.1016/j.gloplacha.2013.12.007.

Hall, S. A., Najmuddin, I. J. (1994). Constraints on the tectonic development of the eastern Gulf of Mexico provided by magnetic anomaly data. *Journal of Geophysical Research: Solid Earth*, 99(B4), 7161-7175.

Hames, W. E., Renne, P. R., Ruppel, C. (2000). New evidence for geologically instantaneous emplacement of earliest Jurassic Central Atlantic magmatic province basalts on the North American margin. *Geology*, 28, 859-862.

Hames, W., McHone, J. G., Renne, P., Ruppel, C. (2003). The Central Atlantic magmatic province: Insights from fragments of Pangea. *GMS*, *136*.

Hassan, M. A. H., Klitzke, P., & Franke, D. (2020). The magma-poor Somalian continental margin: Lower crustal boudinage and mantle exhumation. *Marine Geology*, *430*, 106358.

Heatherington, A. L., Mueller, P. A. (1999). Lithospheric sources of North Florida, USA tholeiites and implications for the origin of the Suwannee terrane. *Lithos*, 46, 215-233.

Heatherington, A. L., Mueller, P. A. (2003). Mesozoic igneous activity in the Suwannee terrane, southeastern USA: petrogenesis and Gondwanan affinities. *Gondwana Research*, 6, 296-311.

Heffner, D. M. (2013). *Tectonics of the South Georgia rift* (Doctoral dissertation, University of South Carolina).

Hinz, K., Neben, S., Schreckenberger, B., Roeser, H. A., Block, M., De Souza, K. G., Meyer, H. (1999). The Argentine continental margin north of 48 S: sedimentary successions, volcanic activity during breakup. *Marine and Petroleum Geology*, 16, 1-25.

Horn, B. W., Pindell, J., Steffensen, C., Graham, R. (2017). New hydrocarbon plays in the Gulf of Mexico–Potential of Jurassic clastic plays on both the Yucatán and Florida margins. In *AAPG Annual Convention*

and Exhibition.**Horton** Jr, J. W., Drake, A. A., Rankin, D. W. (1989). Tectonostratigraphic terranes and their Paleozoic boundaries in the central and southern Appalachians. *Geological Society of America Special Papers*, 230, 213-245.

Hudec, M. R., Norton, I. O., Jackson, M. P., Peel, F. J. (2013). Jurassic evolution of the Gulf of Mexico salt basin. *AAPG bulletin*, 97(10), 1683-1710.

Hudec, M. R., Norton, I. O. (2019). Upper Jurassic structure and evolution of the Yucatán and Campeche subbasins, southern Gulf of Mexico. *AAPG Bulletin*, 103, 1133-1151.

Huismans, R. S. Beaumont, C. (2008). Complex rifted continental margins explained by dynamical models of depth-dependent lithospheric extension. *Geology,* 36, 163-166. doi: 10.1130/G24231A.1.

Huismans, R., Beaumont, C. (2011). Depth-dependent extension, two-stage breakup and cratonic underplating at rifted margins. *Nature*, 473(7345), 74-78.

Imbert, P., Philippe, Y. (2005). The Mesozoic opening of the Gulf of Mexico — Part 2: Integrating seismic and magnetic data into a general opening model: 25th Annual Bob F. Perkins Research Conference: Petroleum Systems of Divergent Continental Margin Basins, 1151–1189.

Jammes, S., Huismans, R. S. (2012). Structural styles of mountain building: Controls of lithospheric rheologic stratification and extensional inheritance. *Journal of Geophysical Research: Solid Earth*, 117(B10).

Keen, C. E., Dickie, K., Dafoe, L. T. (2018). Structural characteristics of the ocean-continent transition along the rifted continental margin, offshore central Labrador. *Marine and Petroleum Geology*, *89*, 443–463. https://doi.org/10.1016/j.marpetgeo.2017.10.012

Klitgord, K., Popenoe. P., Schouten. H. (1984). Florida: A Jurassic transform plate boundary. Journal of Geophysical Research, *89*, 7753-7772.

Koopmann, H., Franke, D., Schreckenberger, B., Schulz, H., Hartwig, A., Stollhofen, H., di Primio, R. (2014). Segmentation and volcano-tectonic characteristics along the SW African continental margin, South Atlantic, as derived from multichannel seismic and potential field data. *Marine and Petroleum Geology*, 50, 22-39.

Lau, K. W. H., Nedimović, M. R., Louden, K. E. (2019). Along-Strike Variations in Structure of the Continent-Ocean Transition at the Northeastern Nova Scotia Margin From Wide-Angle Seismic Observations. *Journal of Geophysical Research: Solid Earth*, *124*(3), 3172–3196. https://doi.org/10.1029/2018JB016894

Lawton, T. F., Bradford, I. A., Vega, F. J., Gehrels, G. E., Amato, J. M. (2009). Provenance of Upper Cretaceous–Paleogene sandstones in the foreland basin system of the Sierra Madre Oriental, northeastern Mexico, and its bearing on fluvial dispersal systems of the Mexican Laramide province: *Geological Society of America Bulletin,* 121, 820–836, doi:10.1130/ B26450.1.

Lawton, T.F. (2018). Pennsylvanian-Triassic magmatic flux in northern Mexico as indicated by detrital zircon data from Triassic-Lower Cretaceous strata, in Geological Society of America Rocky Mountain/Cordilleran Joint Section Meeting, Flagstaff, Arizona, USA, 15–17 May

Legeay, E., Ringenbach, J. C., Callot, J. P. (2020). Along-Strike Variation of Halokinesis and Structural Inheritance Along the West African Salt Basin, South Atlantic. In *EGU General Assembly Conference Abstracts* (p. 12996).

Liao, J. Gerya, T. (2014). Influence of lithospheric mantle stratification on craton extension: Insight from two-dimensional thermomechanical modeling. *Tectonophysics,* 631, 50–64. https://doi.org/10.1016/j.tecto.2014.01.020.

Lin, P. (2018). *Crustal structure and tectonostratigraphic evolution of the eastern Gulf of Mexico Basin* (Doctoral dissertation).

Lin, P., Bird, D. E., Mann, P. (2019). Crustal structure of an extinct, late Jurassic-to-earliest Cretaceous spreading center and its adjacent oceanic crust in the eastern Gulf of Mexico. *Marine Geophysical Research*, 40, 395-418.

Liu, M., Filina, I., Mann, P. (2019). Crustal structure of Mesozoic rifting in the northeastern Gulf of Mexico from integration of seismic and potential fields data. *Interpretation*, 7(4), T857-T867.

Manatschal, G., Nievergelt, P. (1997). A continent-ocean transition recorded in the Err and Platta nappes (Eastern Switzerland). *Eclogae Geologicae Helvetiae*, *90*(1), 3-28.

Manatschal, G., Bernoulli, D. (1999). Architecture and tectonic evolution of nonvolcanic margins: Present-day Galicia and ancient Adria. *Tectonics*, 18(6), 1099-1119.

Manatschal, G. (2004). New models for evolution of magma-poor rifted margins based on a review of data and concepts from West Iberia and the Alps. *International Journal of Earth Sciences*, 93(3), 432-466.

Marton, G., Buffler, R. T. (1994). Jurassic reconstruction of the Gulf of Mexico Basin. *International Geology Review*, 36(6), 545-586.

Marzoli, A., Jourdan, F., Puffer, J. H., Cuppone, T., Tanner, L. H., Weems, R. E., Bertrand, H., Cirilli, S., Bellieni, G., De Min, A. (2011). Timing and duration of the Central Atlantic magmatic province in the Newark and Culpeper basins, eastern USA. *Lithos*, 122(3-4), 175-188.

Maus, S., Barckhausen, U., Berkenbosch, H., Bournas, N., Brozena, J., Childers, V., ... & Gaina, C. (2009). EMAG2: A 2–arc min resolution Earth Magnetic Anomaly Grid compiled from satellite, airborne, and marine magnetic measurements. *Geochemistry, Geophysics, Geosystems*, 10(8).

May, P. R. (1971). Pattern of Triassic-Jurassic diabase dikes around the North Atlantic in the context of predrift position of the continents. *Geological Society of America Bulletin*, 82(5), 1285-1292.

McCarthy, A., Falloon, T. J., Sauermilch, I., Whittaker, J. M., Niida, K., & Green, D. H. (2020). Revisiting the Australian-Antarctic ocean-continent transition zone using petrological and geophysical

characterization of exhumed subcontinental mantle. *Geochemistry, Geophysics, Geosystems*, *21*(7), e2020GC009040.

Mercier de Lépinay, M., Loncke, L., Basile, C., Roest, W.R., Patriat, M., Maillard, A. De Clarens, P. (2016). Transform continental margins - Part 2: a worldwide review. *Tectonophysics* 693. http://dx.doi.org/10.1016/j.tecto.2016.05.038.

Messager, G., Blanc, N., Rodrigues, N., Demichelis, J., Skogseid, J., Hansen, A. (2019). The early stages of opening of the Gulf of Mexico- shaping the margins. In: Petroleum Geology of Mexico and the Northern Caribbean, Abstracts Book, The Geological Society

Mickus, K., Stern, R. J., Keller, G. R., Anthony, E. Y. (2009). Potential field evidence for a volcanic rifted margin along the Texas Gulf Coast. *Geology*, 37(5), 387-390.

Milliken, J.V. (1988). Late Paleozoic and early Mesozoic geologica evolution of the ARKLATEX Area. M.A. Thesis, Rice University, Houston, Texas, USA.

Minguez, D., Gerald Hensel, E., Johnson, E. A. (2020). A fresh look at Gulf of Mexico tectonics: Testing rotations and breakup mechanisms from the perspective of seismically constrained potential-fields modeling and plate kinematics. *Interpretation*, 8(4), SS31-SS45.

Miranda-Madrigal, E., Chávez-Cabello, G. (2021). Regional geological analysis of the southern deep Gulf of México and northern Yucatán Shelf. *Geological Society, London, Special Publications*, *504*(1), 183-202.

Miranda-Peralta, L. R., Cárdenas Alvarado, A., Maldonado Villalón, R., Reyes Tovar, E., Ruiz Morales, J., Williams Rojas, C. (2014). Play hipotético pre-sal en aguas profundas del Golfo de México. *Ingeniería petrolera*, 54(5), 256-266.

Mohn, G., Manatschal, G., Beltrando, M., Masini, E., & Kusznir, N. (2012). Necking of continental crust in magma-poor rifted margins: Evidence from the fossil Alpine Tethys margins. *Tectonics*, *31*(1).

Mortimer, E. J., Gouiza, M., Paton, D. A., Stanca, R., Rodriguez, K., Hodgson, N., & Hussein, A. A. (2020). Architecture of a magma poor passive margin–Insights from the Somali margin. *Marine Geology*, *428*, 106269.

Museur, T., Graindorge, D., Klingelhoefer, F., Roest, W. R., Basile, C., Loncke, L., Sapin, F. (2021). Deep structure of the Demerara Plateau: From a volcanic margin to a Transform Marginal Plateau. *Tectonophysics*, 803, 228645.

Nguyen, L. C., Mann, P. (2016). Gravity and magnetic constraints on the Jurassic opening of the oceanic Gulf of Mexico and the location and tectonic history of the Western Main transform fault along the eastern continental margin of Mexico. *Interpretation*, 4(1), SC23-SC33.

Nirrengarten, M., Manatschal, G., Yuan, X., Kusznir, N. Maillot, B. (2016). Application of the critical Coulomb wedge theory to hyperextended, magma-poor rifted margins. *Earth and Planetary Science Letters* **442**, 121-132.

Olson, H. C., Snedden, J. W., Cunningham, R. (2015). Development and application of a robust chronostratigraphic framework in Gulf of Mexico Mesozoic exploration. *Interpretation*, *3*(2), SN39-SN58.

Pascoe, R., Nuttall, P., Dunbar, D., Bird, D. (2016). Constraints on the timing of continental rifting and oceanic spreading for the Mesozoic Gulf of Mexico Basin. *Mesozoic of the gulf rim and beyond: New progress in science and exploration of the Gulf of Mexico Basin, Gulf Coast Section SEPM Foundation*, 81-122.

Pavlis, N.K., Holmes S.A., Kenyon S.C., Factor J.K., 2008. An Earth Gravitational Model to degree 2160: EGM2008. General Assembly of the European Geosciences Union, Vienna, Austria, April 13-18, 2008.

Peel, F. J., Travis, C. J., & Hossack, J. R. (1995). Genetic structural provinces and salt tectonics of the Cenozoic offshore US Gulf of Mexico: A preliminary analysis.

Peel, F. (2019). The Louann Salt of the Gulf of Mexico: How Long Does it Take to Deposit a Giant Salt Deposit?. In *2019 AAPG Annual Convention and Exhibition*.

Pereira, R., Alves, T. M., Mata, J. (2017). Alternating crustal architecture in West Iberia: a review of its significance in the context of NE Atlantic rifting. *Journal of the Geological Society*, *174*(3), 522-540.

Pereira, R., & Alves, T. M. (2011). Margin segmentation prior to continental break-up: A seismic–stratigraphic record of multiphased rifting in the North Atlantic (Southwest Iberia). *Tectonophysics*, *505*(1-4), 17-34.

Péron-Pinvidic, G., Manatschal, G., Minshull, T. A., Sawyer, D. S. (2007). Tectonosedimentary evolution of the deep Iberia-Newfoundland margins: Evidence for a complex breakup history. *Tectonics*, *26*(2).

Péron-Pinvidic, G., Manatschal, G. (2009). The final rifting evolution at deep magma-poor passive margins from Iberia-Newfoundland: a new point of view. *International Journal of Earth Sciences*, *98*(7), 1581-1597.

Péron-Pinvidic, G., Manatschal, G., & Osmundsen, P. T. (2013). Structural comparison of archetypal Atlantic rifted margins: A review of observations and concepts. *Marine and petroleum geology*, *43*, 21-47.

Péron-Pinvidic, G., Manatschal, G., Masini, E., Sutra, E., Flament, J. M., Haupert, I., Unternehr, P. (2017). Unravelling the along-strike variability of the Angola–Gabon rifted margin: a mapping approach. *Geological Society, London, Special Publications*, 438(1), 49-76.

Péron-Pinvidic, G., Osmundsen, P. T. (2018). The Mid Norwegian-NE Greenland conjugate margins: Rifting evolution, margin segmentation, and breakup. *Marine and Petroleum Geology*, 98, 162-184.

Péron-Pinvidic, G, Manatschal, G. and the "IMAGinING RIFTING" Workshop Participants. (2019). Rifted Margins: State of the Art and Future Challenges. *Front. Earth Sci.* **7**. doi: 10.3389/feart.2019.00218.

Pilcher, R. S., Murphy, R. T., Ciosek, J. M. (2014). Jurassic raft tectonics in the northeastern Gulf of Mexico. *Interpretation*, *2*(4), SM39-SM55.

Pindell, J., Dewey, J. F. (1982). Permo-Triassic reconstruction of western Pangea and the evolution of the Gulf of Mexico/Caribbean region. *Tectonics*, *1*(2), 179-211.

Pindell, J. L. (1985). Alleghenian reconstruction and subsequent evolution of the Gulf of Mexico, Bahamas, and Proto-Caribbean. *Tectonics*, *4*(1), 1-39.

Pindell, J. L., Kennan, L. (2001). Kinematic evolution of the Gulf of Mexico and Caribbean. In *Transactions of the Gulf Coast Section Society of Economic Paleontologists and Mineralogists (GCSSEPM) 21st Annual Bob F. Perkins Research Conference, Petroleum Systems of Deep-Water Basins, Houston, Texas, December* (pp. 2-5).

Pindell, J. L., Kennan, L. (2009). Tectonic evolution of the Gulf of Mexico, Caribbean and northern South America in the mantle reference frame: an update. *Geological Society, London, Special Publications*, *328*(1), 1-55.

Pindell, J., Radovich, B., Horn, B. (2011). Western Florida: A new exploration frontier in the eastern Gulf of Mexico. *GeoExPro*, *8*, 37-40.

Pindell, J., Graham, R., & Horn, B. (2014). Rapid outer marginal collapse at the rift to drift transition of passive margin evolution, with a Gulf of Mexico case study. *Basin Research*, *26*(6), 701-725.

Pindell, J., Radovich, B., Haire, D. H., Goswami, A., Dinc, G., & Horn, B. (2015). Structure maps of the top-rift unconformity/oceanic crust and top Cretaceous surfaces, and the Oxfordian rift-drift reconstruction, Gulf of Mexico.

Pindell, J., Miranda, C. E., Cerón, A., Hernandez, L. (2016). Aeromagnetic map constrains Jurassic-Early cretaceous synrift, break up, and rotational seafloor spreading history in the Gulf of Mexico. *Mesozoic of*

the Gulf Rim and beyond: New progress in science and exploration of the Gulf of Mexico Basin: SEPM Society for Sedimentary Geology, *35*, 123-153.

Pindell, J.L., Graham, R., Horn, B.W. (2018). Role of outer marginal collapse on salt deposition in the eastern Gulf of Mexico, Campos and Santos basins. *Geological Society, London, Special Publications*, 476, 317–331, https://doi.org/10.1144/SP476.4

Pindell, J.L., B. Weber, W-H. Elrich, S.P. Cossey, M.R. Bitter, R.S. Molina, R.H. Graham, and R.N. Elrich (2019). Strontium isotope dating of evaporates and the breakup of the Gulf of Mexico and proto-Caribbean seaway (abs.): AAPG annual convention and exhibition, 19-22 May, San Antonio, Texas.

Pindell, J., Villagómez, D., Molina-Garza, R., Graham, R., & Weber, B. (2021). A revised synthesis of the rift and drift history of the Gulf of Mexico and surrounding regions in the light of improved age dating of the Middle Jurassic salt. *Geological Society, London, Special Publications*, *504*(1), 29-76.

Pollastro, R. M., C. J. Schenk, and R. R. Charpentier, 2001, Assessment of Undiscovered Oil and Gas in the Onshore and State Waters Portion of the South Florida Basin, Florida – USGS Province 50: National Assessment of Oil and Gas Project: Petroleum Systems and Assessment of South Florida Basin, U.S. Geological Survey, Digital Data Series 69-A, 1–17.

Pulham A.J., F.J. Peel, T. Rives, B. Delph, J-F. Salel, J, Wu, and R. Requejo, (2019). The age of the Louann Salt; insights from historic isotopic analyses in salt stocks from the onshore interior salt basins of the Northern Gulf of Mexico: GCSSEPM Foundation 37th Annual Perkins-Rosen Research Conference

Ranero, C. R., Pérez-Gussinyé, M. (2010). Sequential faulting explains the asymmetry and extension discrepancy of conjugate margins. *Nature*, *468*(7321), 294-299.

Reuber, K. R., Pindell, J., Horn, B. W. (2016). Demerara Rise, offshore Suriname: Magma-rich segment of the Central Atlantic Ocean, and conjugate to the Bahamas hot spot. *Interpretation*, *4*(2), T141-T155.

Rey, P. F., Teyssier, C., Whitney, D. L. (2009). Extension rates, crustal melting, and core complex dynamics. *Geology* **37**, 391–394. https://doi.org/10.1130/G2546 0A.1.

Rives, T., Pierin, A. R., Pulham, A. J., Salel, J. F., Wu, J., Duarte, A., Magnier, B. (2019). The Sakarn Series: A Proposed New Middle Jurassic Stratigraphic Interval from the Offshore Eastern Gulf of Mexico. GCSSEPM Foundation 37th Annual Perkins-Rosen Research Conference

Rowan, M. G., Kligfield, R. (1989). Cross section restoration and balancing as aid to seismic interpretation in extensional terranes. *AAPG bulletin*, *73*(8), 955-966.

Rowan, M. G. (2014). Passive-margin salt basins: Hyperextension, evaporite deposition, and salt tectonics. *Basin Research*, *26*(1), 154-182.

Rowan, M. (2018). The South Atlantic and Gulf of Mexico salt basins: crustal thinning, subsidence and accommodation for salt and pre-salt strata. Geological Society, London, Special Publications, 476, 333-363, 17 https://doi.org/10.1144/SP476.6

Salvador, A. (1987). Late Triassic-Jurassic paleogeography and origin of Gulf of Mexico basin. *AAPG Bulletin*, *71*(4), 419-451.

Salvador, A. (1991). Triassic-Jurassic. *The Gulf of Mexico Basin: Boulder, Colorado, Geological Society of America, Geology of North America, v. J*, 131-180.

Sandwell, D. T., Müller, R. D., Smith, W. H., Garcia, E., Francis, R. (2014). New global marine gravity model from CryoSat-2 and Jason-1 reveals buried tectonic structure. *Science*, *346*(6205), 65-67.

Sapin, F., Ringenbach, J. C., Clerc, C. (2021). Rifted margins classification and forcing parameters. *Scientific Reports*, *11*(1), 1-17.

Snedden, J. W., J. Virdell, T. L. Whiteaker, and P. Ganey-Curry (2016). A basin-scale perspective on Cenomanian–Turonian (Cretaceous) depositional systems, greater Gulf of Mexico (USA): Interpretation, 4, SC1–SC22, doi:10.1190/INT-2015-0082.1.

Snedden, J. W., Norton, I., Hudec, M., Eljalafi, A., Peel, F. (2018). Paleogeographic reconstruction of the Louann salt basin in the Gulf of Mexico (abs.): AAPG Annual Convention and Exhibition, Salt Lake City, Utah, May 20–23, 2018.

Snedden, J. W., Galloway, W. E. (2019). *The Gulf of Mexico Sedimentary Basin: Depositional Evolution and Petroleum Applications*. Cambridge University Press.

Snedden, J.W., Hudec, M.R., Peel, F. (2019). Paleogeographic reconstruction of the Louann Salt Basin. In: Fiduk, J.C. and Rosen, N.C. (eds) Salt Tectonics, Associated Processes, and Exploration Potential: Revisited: 1989–2019. Program and Abstracts. Gulf Coast Section SEPM, Houston, TX, 5.

Soto, M., Morales, E., Veroslavsky, G., de Santa Ana, H., Ucha, N., & Rodríguez, P. (2011). The continental margin of Uruguay: Crustal architecture and segmentation. *Marine and Petroleum Geology*, *28*(9), 1676-1689.

Steier, A., Mann, P. (2019). Late Mesozoic gravity sliding and Oxfordian hydrocarbon reservoir potential of the northern Yucatan margin. *Marine and Petroleum Geology*, *103*, 681-701.

Storey, M. L. (2020). *Tectonic Setting, Structure, and Seismic Stratigraphy of the ApalachicolaRift and its Overlying Sag Basin in the Northeastern Gulf of Mexico* (Doctoral dissertation, University of Houston).

Sutra, E., Manatschal, G. (2012) How does the continental crust thin in a hyperextended rifted margin? Insights from the Iberia margin. *Geology* **40**, 139-142

Sutra, E., Manatschal, G., Mohn, G. Unternehr, P. (2013). Quantification and restoration of extensional deformation along the Western Iberia and Newfoundland rifted margins. *Geochemistry, Geophysics, Geosystems* **14**, 2575-2597

Tavares, A. C., de Castro, D. L., Bezerra, F. H., Oliveira, D. C., Vannucchi, P., Iacopini, D., ... & Vital, H. (2020). The Romanche fracture zone influences the segmentation of the equatorial margin of Brazil. *Journal of South American Earth Sciences*, 102738.

Tchernychev, M. (1998). MAGPICK-Magnetic Map&Profile Processing User Guide.

Tetreault, J. L., Buiter, S. J. H. (2018). The influence of extension rate and crustal rheology on the evolution of passive margins from rifting to break-up. *Tectonophysics*, *746*, 155-172.

Tew, B. H., Mink, R. M., Mann, S. D., Bearden, B. L., & Mancini, E. A. (1991). Geologic framework of Norphlet and pre-Norphlet strata of the onshore and offshore eastern Gulf of Mexico area.

Tsikalas, F., Faleide, J. I., & Kusznir, N. J. (2008). Along-strike variations in rifted margin crustal architecture and lithosphere thinning between northern Vøring and Lofoten margin segments off mid-Norway. *Tectonophysics*, *458*(1-4), 68-81.

Tugend, J., Manatschal, G., Kusznir, N. J., Masini, E. (2015). Characterizing and identifying structural domains at rifted continental margins: application to the Bay of Biscay margins and its Western Pyrenean fossil remnants. *Geological Society, London, Special Publications*, *413*(1), 171-203.

Turner, J. P., Rosendahl, B. R., Wilson, P. G. (2003). Structure and evolution of an obliquely sheared continental margin: Rio Muni, West Africa. *Tectonophysics*, *374*(1-2), 41-55.

Unternehr, P., Péron-Pinvidic, G., Manatschal, G., Sutra, E. (2010). Hyper-extended crust in the South Atlantic: in search of a model. *Petroleum Geoscience*, *16*(3), 207-215.

Van Avendonk, H. J., Christeson, G. L., Norton, I. O., Eddy, D. R. (2015). Continental rifting and sediment infill in the northwestern Gulf of Mexico. *Geology*, *43*(7), 631-634.

Withjack, M. O., Schlische, R. W., Olsen, P. E. (1998). Diachronous rifting, drifting, and inversion on the passive margin of central eastern North America: an analog for other passive margins. *AAPG bulletin*, *82*(5), 817-835.

Wiley, K. S. (2017). Provenance of Syn-rift Clastics in the Eastern Gulf of Mexico: Insight from U–Pb Detrital Zircon Geochronology and Thin Sections: MS thesis, West Virginia University, 194 p

Wood, G. D., Benson Jr, D. G. (2000). The north american occurrence of the algal coenobium plaesiodictyon'. paleogeographic, paleoecologic, and biostratigraphic importance in the Triassic. *Palynology*, *24*(1), 9-20.

Zhao, F., Alves, T. M., Xia, S., Li, W., Wang, L., Mi, L., ... & Fan, C. (2020). Along-strike segmentation of the South China Sea margin imposed by inherited pre-rift basement structures. *Earth and Planetary Science Letters*, *530*, 115862.

Zwaan, F., Schreurs, G., Naliboff, J., & Buiter, S. J. (2016). Insights into the effects of oblique extension on continental rift interaction from 3D analogue and numerical models. *Tectonophysics*, *693*, 239-260.

Figure captions

Fig. 1. A) Vertical gravity gradient map (Sandwell et al., 2014) with location of the seismic-based cross-sections in this work (WGS84 Datum, UTM coordinates, 15N). The limit of the oceanic crust (LOC) is mapped from Hudec et al. (2013) and Sandwell et al. (2014) and refined considering the seismic profiles used in this study. The extinct spreading ridge and fracture zones in the oceanic crust are from Nguyen and Mann (2016) whereas the extent of the Louann Salt is from Rowan (2014). The rotation pole is from the single pole model by Pindell and Kennan (2001) and agrees well with the finite rotation pole for early Oxfordian from Pindell et al. (2016). Location of the deep seismic refraction profiles Gumbo-1 to Gumbo-4 (G1 to G4; Christeson et al., 2014; Van Avendonk et al., 2015; Eddy et al., 2014, 2018) is also shown. Mapping of early rifts (phase-1 rifting) is shown (from Pindell et al., 2015, 2021 and Storey, 2020 for the Florida offshore and from Miranda-Peralta et al., 2014 for the central-western Yucatan margin). SGB = South Georgia Basin (SGB), AB = Apalachicola Basin, TA = Tampa Arch. **B)** Restoration of cross-section traces to the onset of oceanic spreading time. Restoration was done using the rotation pole in Fig. 1a and applying a clockwise rotation of 31 º to the Yucatan block (following rotation values in Pindell and Kennan, 2001).

Fig. 2. Synthetic stratigraphic column in the Gulf of Mexico. Dominant lithologies, interpreted seismic horizons and main tectonic events affecting the Gulf of Mexico evolution are shown (see references in the text).

Fig. 3. Correlation between seismic facies and reflection characters and the main horizons interpreted in this study. The columns are enlargements of representative portions of the interpreted seismic lines (see location in figures 4, 7 and 11).

Fig. 4. South Florida- East Yucatan cross-section. See location in Fig. 1. The profile is a merged profile of ION-GXT PrSDM lines FL1-7200 and MX1-420. MOR indicates location of the mid oceanic ridge. LOC = Limit of the Oceanic Crust. Dashed Moho and top continental basement horizons indicate the zones where related seismic reflections are not well imaged.

Fig. 5. East Yucatan cross-section. See location in Fig. 1. CD = Coupled Domain. LOC = Limit of the oceanic crust. Dashed Moho and top continental basement horizons indicate the zones where related seismic reflections are not well imaged.

Fig. 6. South Florida cross-section. See location in Fig. 1. LOC = Limit of the oceanic crust. Dashed Moho and top continental basement horizons indicate the zones where related seismic reflections are not well imaged.

Fig. 7. North Florida- Central Yucatan cross-section. See location in Fig. 1. The profile is a merged profile of ION-GXT lines FL1-6400, GSR1-6400 and MX1-390. LOC = Limit of the Oceanic Crust; LCC = Limit of the Continental Crust; OCT = Ocean-Continent Transition. Dashed Moho and top continental basement horizons indicate the zones where related seismic reflections are not well imaged.

Fig. 8. Central Yucatan cross-section. See location in Fig. 1. LOC = Limit of the Oceanic Crust; LCC = Limit of the Continental Crust; OCT = Ocean-Continent Transition. Dashed Moho and top continental basement horizons indicate the zones where related seismic reflections are not well imaged.

Fig. 9. North Florida cross-section. Florida platform portion. See location in Fig. 1. Dashed Moho and top continental basement horizons indicate the zones where related seismic reflections are not well imaged.

Fig. 10. North Florida cross-section (E-Manatee 3D survey), deepest offshore portion. See location in Fig. 1 and Fig. 7. CD = Coupled domain. LOC = Limit of the Oceanic Crust; LCC = Limit of the Continental Crust; OCT = Ocean-Continent Transition. Dashed Moho and top continental basement horizons indicate the zones where related seismic reflections are not well imaged.

Fig. 11. West Yucatan cross-section. See location in Fig. 1. The profile is tied to the ION-GXT line MX1-360 and it is completed in the offshore Texas with the velocity model across the seismic refraction profile Gumbo-2 (see location in Fig. 1, Eddy et al., 2018). LOC = Limit of the Oceanic Crust; LCC = Limit of the Continental Crust; OCT = Ocean-Continent Transition. Dashed Moho and top continental basement horizons indicate the zones where related seismic reflections are not well imaged.

Fig. 12. West Yucatan cross-section. See location in Fig. 1. LOC = Limit of the Oceanic Crust; LCC = Limit of the Continental Crust; OCT = Ocean-Continent Transition; CD = Coupled Domain. Dashed Moho and top continental basement horizons indicate the zones where related seismic reflections are not well imaged.

Fig. 13. Simplified version of the cross-sections with definition of the main crustal domains. The western cross-section is completed in the North using the Top Basement and the Moho surfaces interpreted from the seismic refraction profile Gumbo-2 (Eddy et al., 2018).

Fig.14. Geometrical restoration using the area balancing method. Numerical values in Tables 1 and 2. In the North Florida cross-section, the upper-middle/lower crust limit was not reliably identified on seismics and the cross-section was not considered for the calculation of extension from upper and middle-lower crust areas separately. The polygons with dashed, orange contours represent the highly intruded, lower crust bodies interpreted along the Gumbo-3 refraction profile (Eddy et al., 2014).

Fig. 15. Crustal domains map for the Gulf of Mexico overlapping the a) Bouguer (Bonvalot et al., 2012) and b) total magnetic intensity (Maus et al., 2009) anomaly maps in the area. The Bouguer gravity map in a) shows Bouguer anomalies from the WGM2012 global model (Bonvalot et al., 2012), obtained from the available Earth global gravity model EGM2008 (Pavlis et al., 2008). They include 1'x1' resolution terrain corrections derived from the ETOPO1 Global relief model (Amante and Eakins, 2009). Bouguer anomalies are computed at the Earth's surface with a 1'x1' resolution and a reference density of 2670 kg/m^3 is used. The total magnetic intensity anomaly map in b) is built using the EMAG2 model (Maus et al., 2009) that has a 2 arc min resolution and compiles satellite, ship and airborne magnetic measurements. Magnetic data are reduced to the pole. Additional maps showing the defined crustal domains over the vertical gravity gradient (Sandwell et al., 2014) and the vertical derivative of total magnetic intensity anomaly (Maus et al., 2009) are included in the Supplementary Material. Data grids were downloaded using GeoMapApp (www.geomapapp.org) and magnetic data were processed (reduction to the pole, vertical derivative) using MagPick software (Tchernychev, 1998). The area between the LCC and the LOC represents the OCT, characterized in previous cross-sections (Figs. 7-13) as an exhumed mantle and/or magmatic domain. The Cretaceous platform boundary is from Pindell et al, (2016). The extent of the Louann Evaporites (halite and anhydrite or mixed anhydrite-halite facies) is indicated in a (from Rowan, 2014; modified in the eastern Gulf of Mexico using Snedden and Galloway, 2019) whereas the inferred areal distribution of pre-salt, syn-rift units is shown in b. Blue lines indicate location of the cross-sections considered in this study, gray traces indicate the location of the Gumbo seismic refraction profiles (Christeson et al., 2014; Van Avendonk et al., 2015; Eddy et al., 2014, 2018). SGB = South Georgia Basin; TALB = Texas-Arkansas-Louisiana Basin. SWA = Small Wavelength Anomalies.

Fig. 16. Diagrams showing the across-strike variation of crustal and sedimentary thicknesses in the three studied cross-sections. Beta factors are also shown (in blue) together with crustal thicknesses (in black). Limits of the crustal domains defined in Fig. 13 are also indicated. Syn-rift thicknesses are

underestimated in b) and c) where we approximated the base of the Louann salt to the top of the syn-rift.

Fig. 17. Schematic evolution of syn-rift sedimentation and crustal extension stages in a) the North Florida and Central-Western Yucatan and b) the South Florida and Eastern Yucatan domains (see location of the reference cross-sections in Fig. 1).

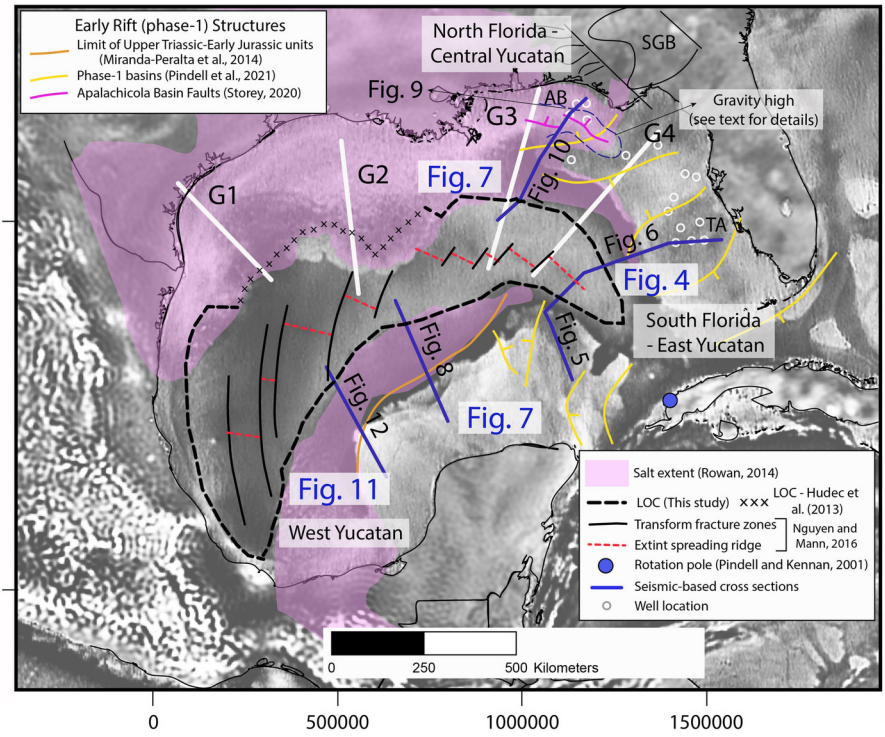
Early Rift (phase-1) Structures
Limit of Upper Triassic-Early Jurassic units (Miranda-Peralta et al., 2014)
Phase-1 basins (Pindell et al., 2021)
Apalachicola Basin Faults (Storey, 2020)
North Florida - Central Yucatan
SGB
Fig. 9
AB
G3
Gravity high (see text for details)
G4
Fig. 10
G1
G2
Fig. 7
Fig. 6
TA
Fig. 4
South Florida - East Yucatan
Fig. 8
Fig. 5
Fig. 2
Fig. 7
Fig. 11
West Yucatan
Salt extent (Rowan, 2014)
LOC (This study)
LOC - Hudec et al. (2013)
Transform fracture zones
Extint spreading ridge
Nguyen and Mann, 2016
Rotation pole (Pindell and Kennan, 2001)
Seismic-based cross sections
Well location
0
250
500 Kilometers
3000000
2000000
0
500000
1000000
1500000

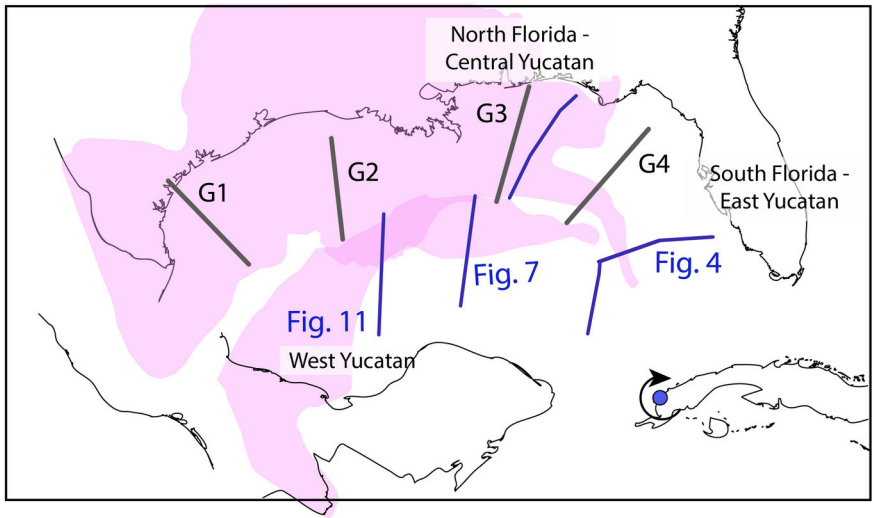
North Florida - Central Yucatan
G3
G2
G1
G4
South Florida - East Yucatan
Fig. 7
Fig. 4
Fig. 11
West Yucatan

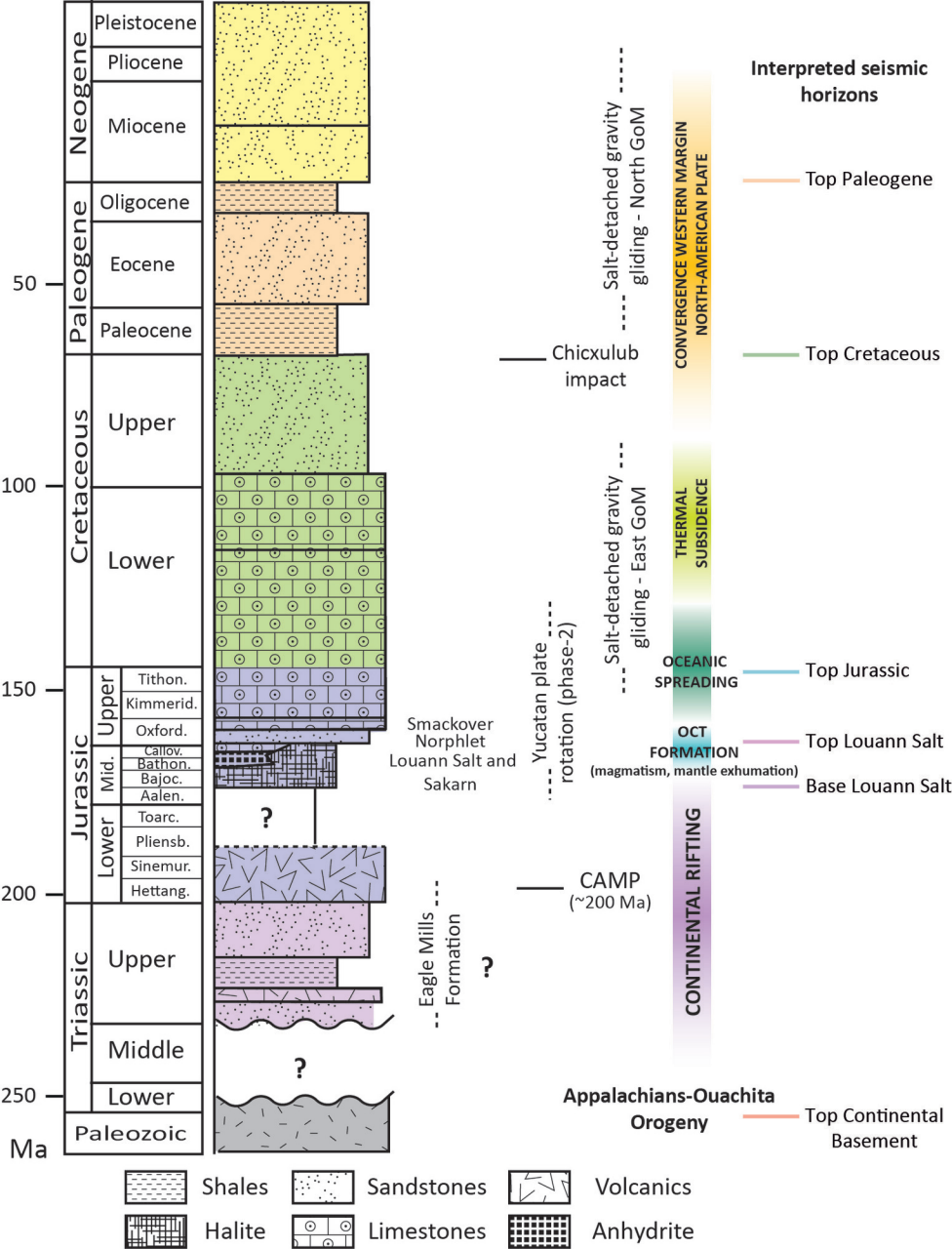
Neogene
Pleistocene
Pliocene
Miocene
Paleogene
Oligocene
Eocene
Paleocene
Cretaceous
Upper
Lower
Jurassic
Upper
Tithon.
Kimmerid.
Oxford.
Mid.
Callov.
Bathon.
Bajoc.
Aalen.
Lower
Toarc.
Pliensb.
Sinemur.
Hettang.
Triassic
Upper
Middle
Lower
Paleozoic
Ma
50
100
150
200
250
Smackover
Norphlet
Louann Salt and
Sakarn
Eagle Mills
Formation
?
?
?
Yucatan plate
rotation (phase-2)
Salt-detached gravity
gliding - East GoM
Salt-detached gravity
gliding - North GoM
Chicxulub
impact
CAMP
(~200 Ma)
CONTINENTAL RIFTING
OCEANIC
SPREADING
OCT
FORMATION
(magmatism, mantle exhumation)
THERMAL
SUBSIDENCE
CONVERGENCE WESTERN MARGIN
NORTH-AMERICAN PLATE
Appalachians-Ouachita
Orogeny
Interpreted seismic
horizons
Top Paleogene
Top Cretaceous
Top Jurassic
Top Louann Salt
Base Louann Salt
Top Continental
Basement
Shales
Sandstones
Volcanics
Halite
Limestones
Anhydrite

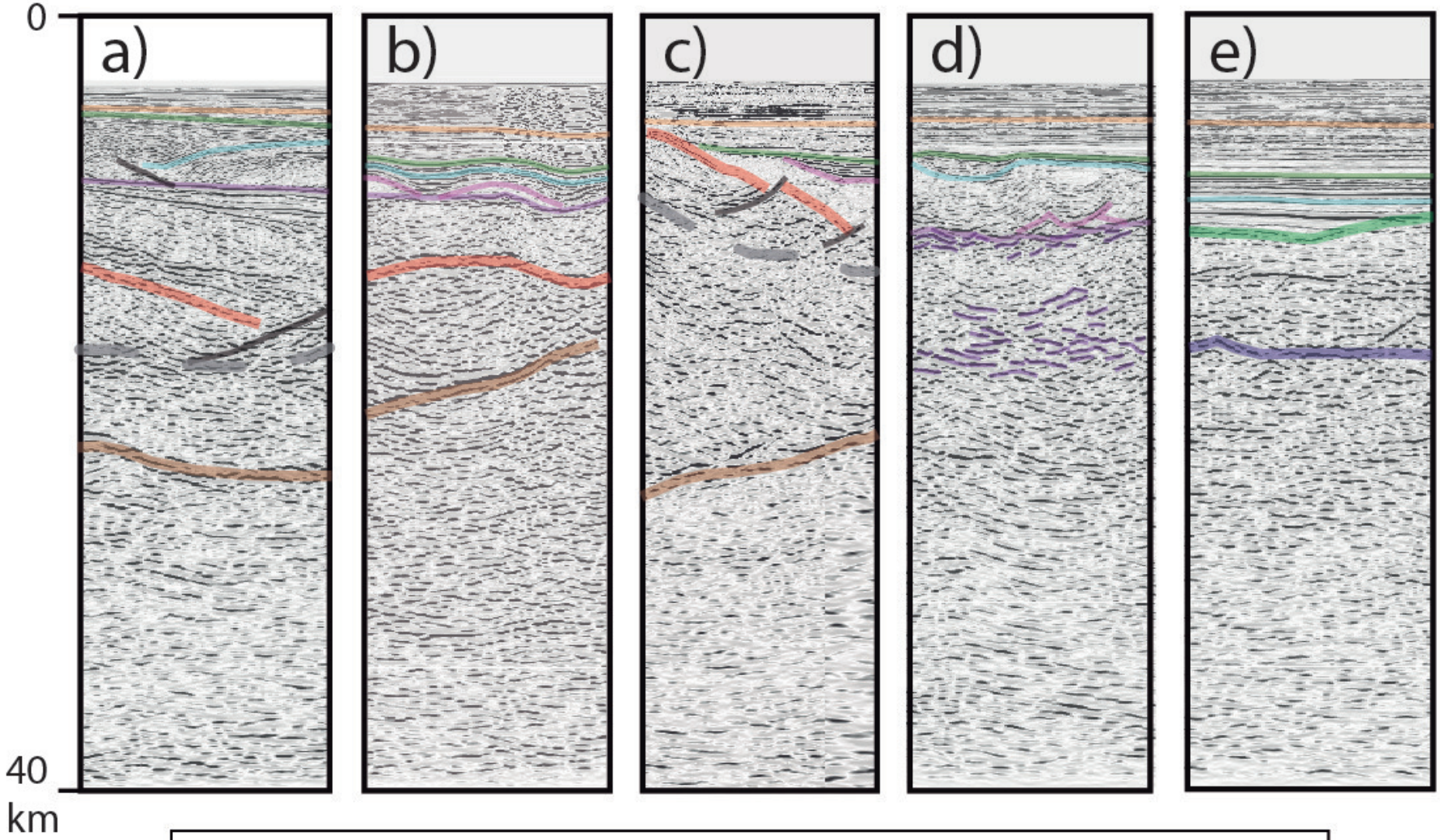
0
a)
b)
c)
d)
e)
40
km
Top Paleogene
Top Cretaceous
Top Jurassic
Top Louann Salt
Base Louann Salt
Interpreted faults
Intrusives/Extrusives at the OCT
Top Continental Basement
Top Oceanic Crust
Upper-Mid/Lower crust
Continental Moho
Oceanic Moho

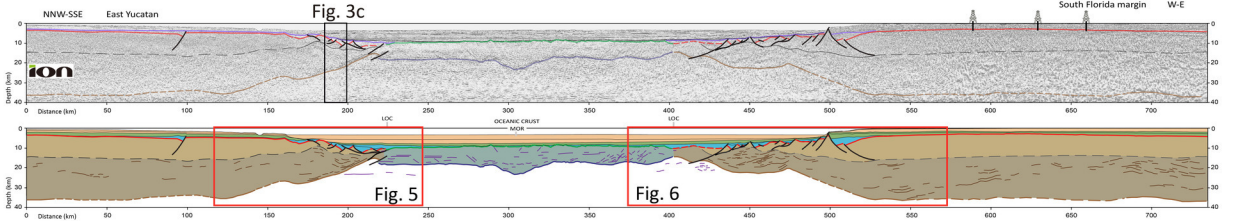
NNW-SSE
East Yucatan
Fig. 3c
South Florida margin
W-E
Depth (km)
Distance (km)
LOC
OCEANIC CRUST
MOR
LOC
Fig. 5
Fig. 6
Upper Continental Crust
Middle/Lower Continental Crust
Oceanic Crust
Cenozoic
Cretaceous
Jurassic
Break-up Unconformity
Top Continental Basement
Top Oceanic Crust
Reflections Oceanic Crust/Mantle
Basement Faults
Continental Moho
Oceanic Moho
Upper-Mid/Lower crust
Reflections M/L Continental Crust

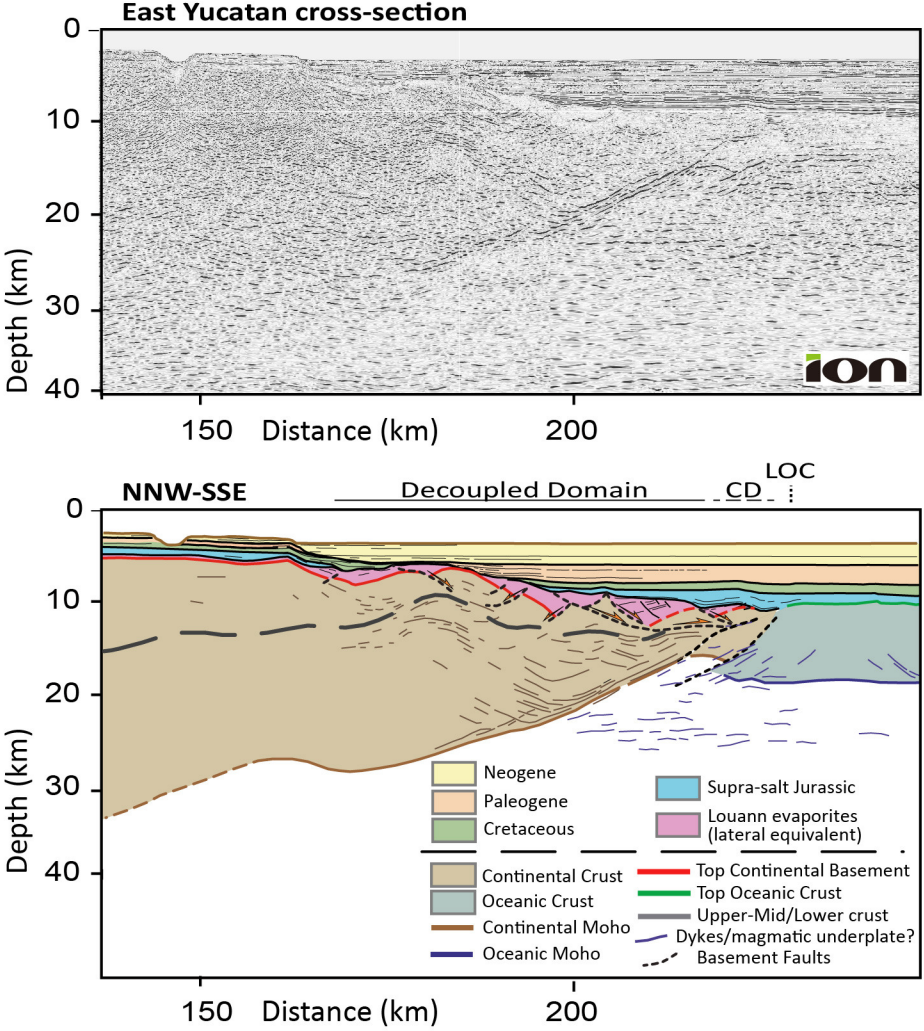
East Yucatan cross-section
0
10
20
30
40
Depth (km)
150
Distance (km)
200
ion
NNW-SSE
Decoupled Domain
CD
LOC
Neogene
Paleogene
Cretaceous
Supra-salt Jurassic
Louann evaporites
(lateral equivalent)
Continental Crust
Oceanic Crust
Continental Moho
Oceanic Moho
Top Continental Basement
Top Oceanic Crust
Upper-Mid/Lower crust
Dykes/magmatic underplate?
Basement Faults

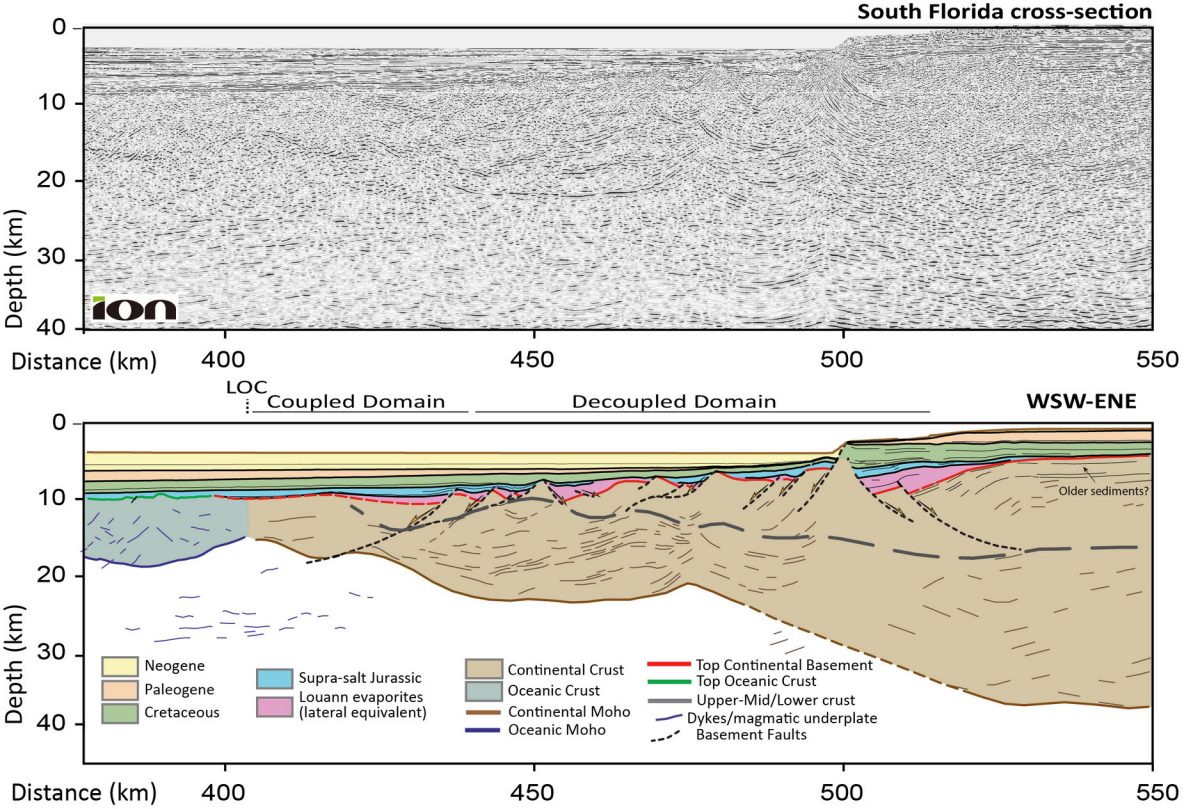
South Florida cross-section
Depth (km)
0
10
20
30
40
Distance (km)
400
450
500
550
LOC
Coupled Domain
Decoupled Domain
WSW-ENE
Older sediments?
Neogene
Paleogene
Cretaceous
Supra-salt Jurassic
Louann evaporites
(lateral equivalent)
Continental Crust
Oceanic Crust
Continental Moho
Oceanic Moho
Top Continental Basement
Top Oceanic Crust
Upper-Mid/Lower crust
Dykes/magmatic underplate
Basement Faults

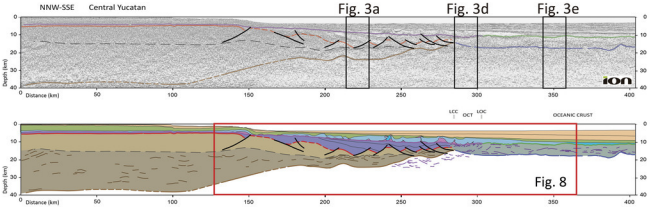

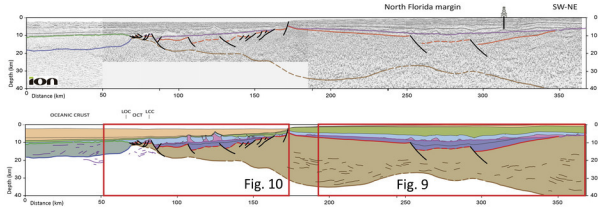

Upper Continental Crust (CC in North Florida)
Middle/Lower Continental Crust
Oceanic Crust
OCT
Cenozoic
Cretaceous
Supra-salt Jurassic
Louann Salt
Pre-salt
Base of the Louann Salt
Top Continental Basement
Top Oceanic Crust
Reflections Oceanic Crust/Mantle
Basement Faults
Continental Moho
Oceanic Moho
Upper-Mid/Lower crust
Reflections M/L Continental Crust

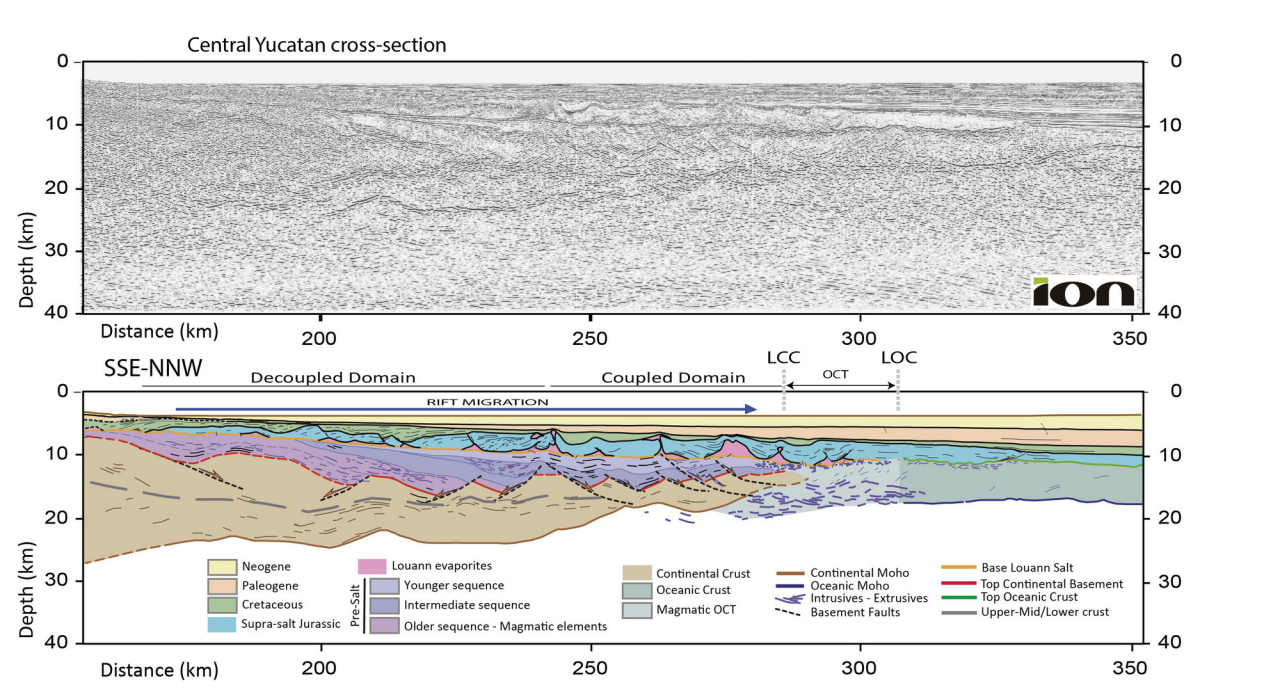
Central Yucatan cross-section
Depth (km)
Distance (km)
0
10
20
30
40
200
250
300
350
SSE-NNW
Decoupled Domain
Coupled Domain
LCC
LOC
OCT
RIFT MIGRATION
Neogene
Paleogene
Cretaceous
Supra-salt Jurassic
Louann evaporites
Pre-Salt
Younger sequence
Intermediate sequence
Older sequence - Magmatic elements
Continental Crust
Oceanic Crust
Magmatic OCT
Continental Moho
Oceanic Moho
Intrusives - Extrusives
Basement Faults
Base Louann Salt
Top Continental Basement
Top Oceanic Crust
Upper-Mid/Lower crust

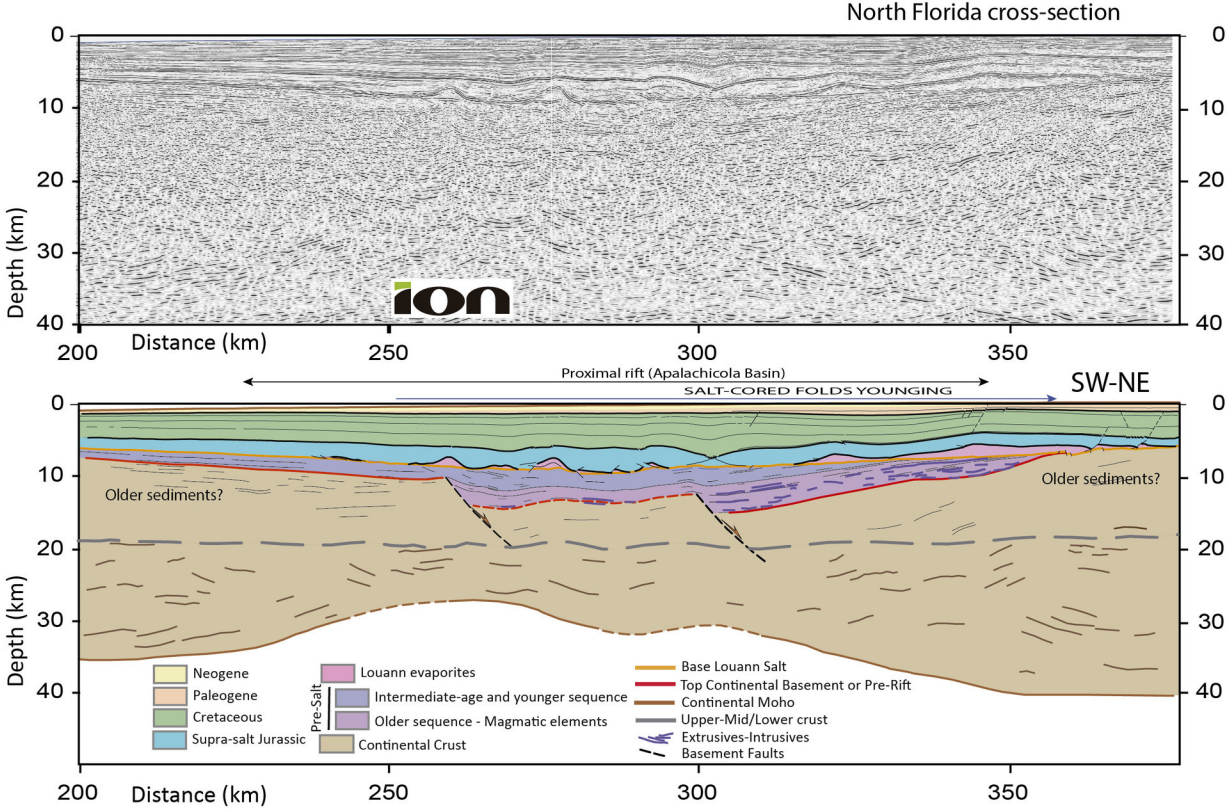
North Florida cross-section
Depth (km)
Distance (km)
Proximal rift (Apalachicola Basin)
SALT-CORED FOLDS YOUNGING
SW-NE
Older sediments?
Older sediments?
Neogene
Paleogene
Cretaceous
Supra-salt Jurassic
Pre-Salt
Louann evaporites
Intermediate-age and younger sequence
Older sequence - Magmatic elements
Continental Crust
Base Louann Salt
Top Continental Basement or Pre-Rift
Continental Moho
Upper-Mid/Lower crust
Extrusives-Intrusives
Basement Faults

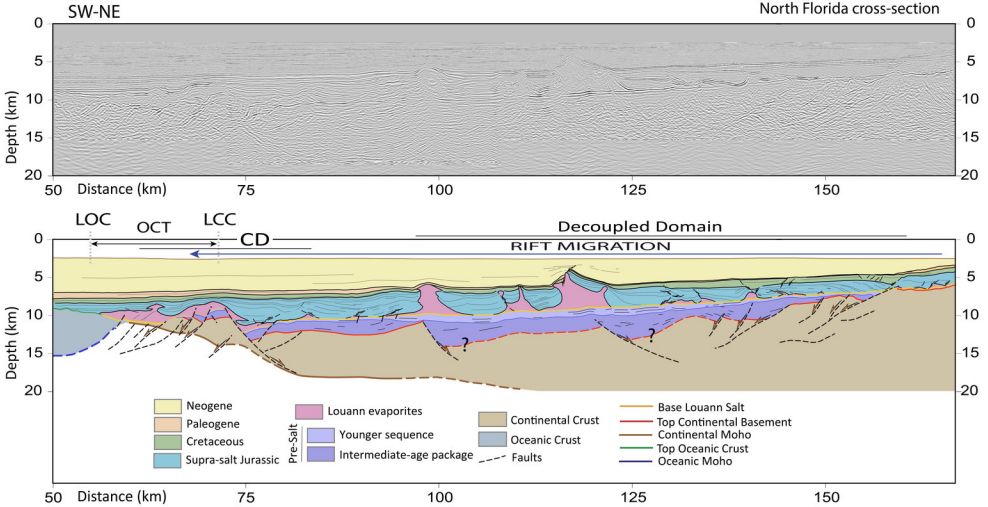
SW-NE
North Florida cross-section
Depth (km)
0
5
10
15
20
50
Distance (km)
75
100
125
150
LOC
OCT
LCC
CD
Decoupled Domain
RIFT MIGRATION
?
?
Neogene
Paleogene
Cretaceous
Supra-salt Jurassic
Pre-Salt
Louann evaporites
Younger sequence
Intermediate-age package
Continental Crust
Oceanic Crust
Faults
Base Louann Salt
Top Continental Basement
Continental Moho
Top Oceanic Crust
Oceanic Moho

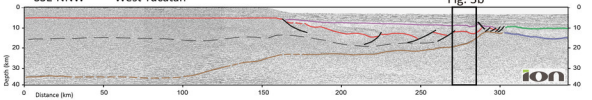

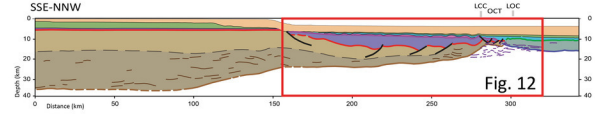

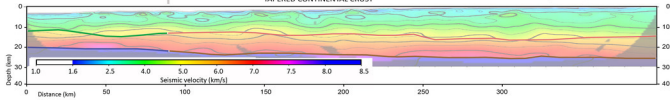

Upper Continental Crust
Middle/Lower Continental Crust
Oceanic Crust

Cenozoic
Cretaceous

Supra-salt Jurassic
Louann Salt
Pre-salt

Base of the Louann Salt
Top Continental Basement
Top Oceanic Crust
Reflections Oceanic Crust/Mantle
Basement Faults

Continental Moho
Oceanic Moho
Upper-Mid/Lower crust
Reflections M/L Continental Crust

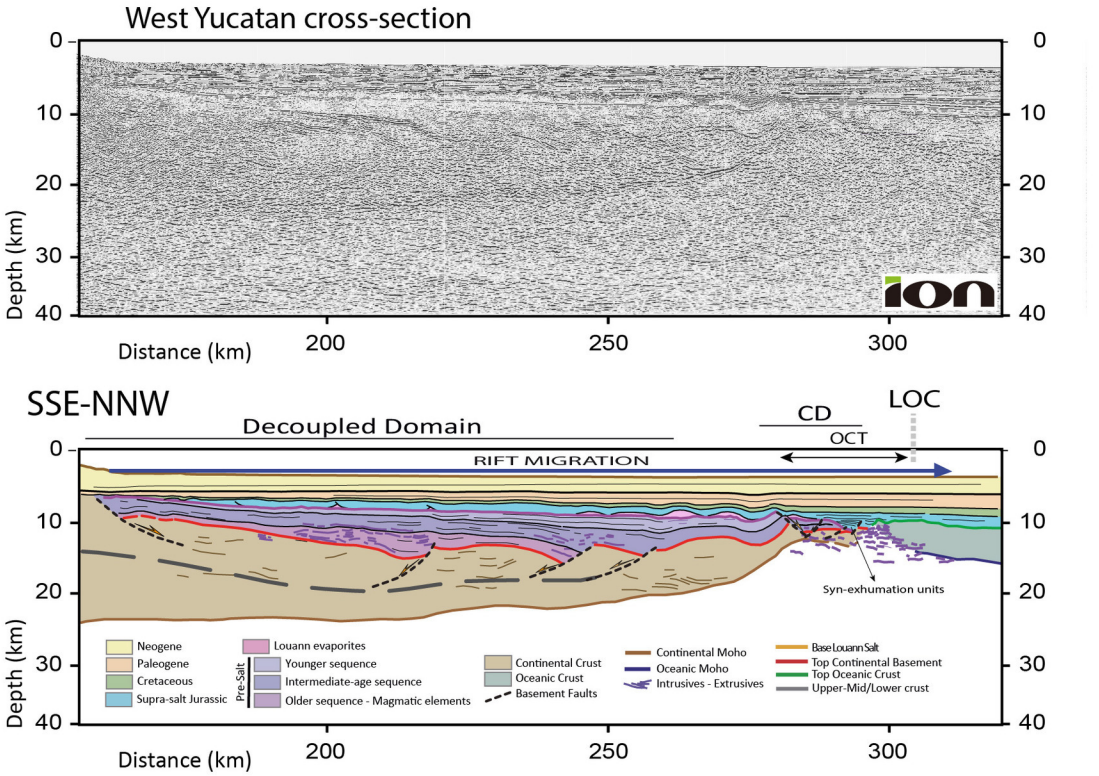
West Yucatan cross-section
Depth (km)
Distance (km)
0
10
20
30
40
200
250
300
ion
SSE-NNW
Decoupled Domain
CD
OCT
LOC
RIFT MIGRATION
Syn-exhumation units
Neogene
Paleogene
Cretaceous
Supra-salt Jurassic
Louann evaporites
Younger sequence
Intermediate-age sequence
Older sequence - Magmatic elements
Pre-Salt
Continental Crust
Oceanic Crust
Basement Faults
Continental Moho
Oceanic Moho
Intrusives - Extrusives
Base Louann Salt
Top Continental Basement
Top Oceanic Crust
Upper-Mid/Lower crust

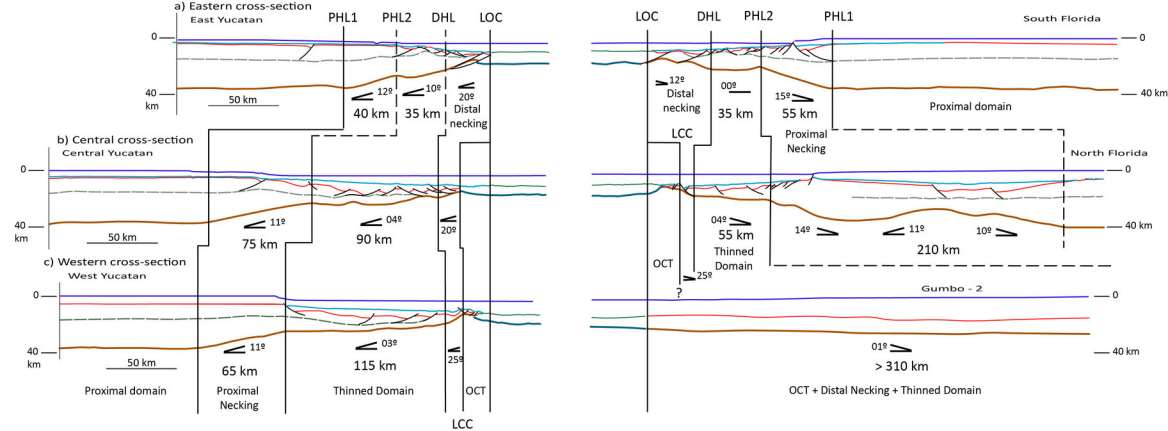

PHL1 = Proximal Moho Hinge Line 1 = proximal limit of the proximal necking; PHL2 = Proximal Moho Hinge Line 2 = distal limit of the proximal necking;
DHL = Distal Moho Hinge Line = Onset of the distal necking LCC = Limit of the Continental Crust LOC = Limit of the Oceanic Crust; OCT = Ocean-Continent Transition

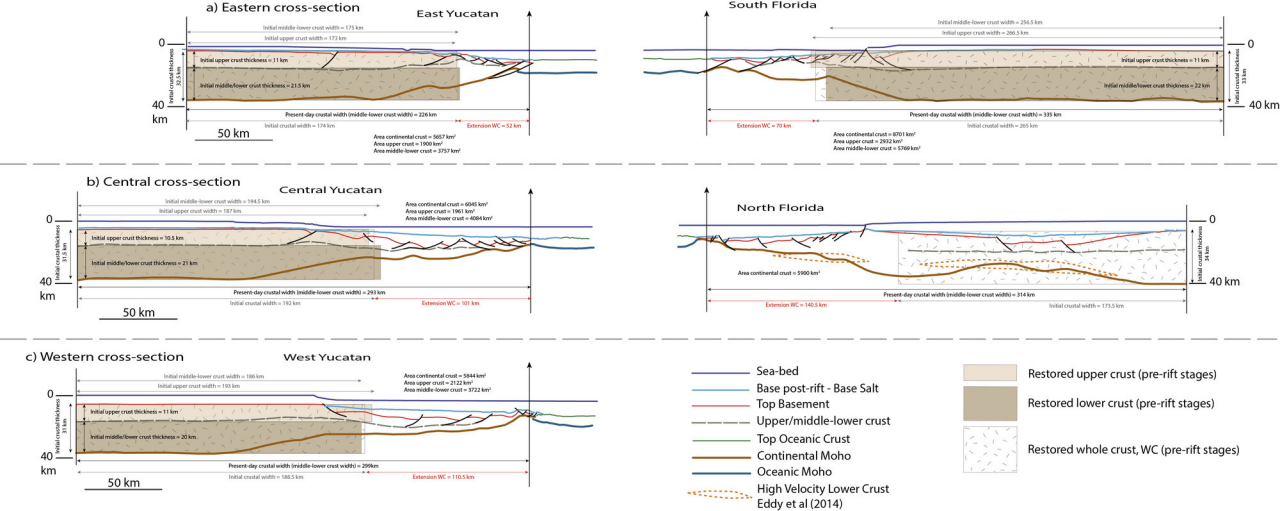
a) Eastern cross-section
East Yucatan
Initial middle-lower crust width = 175 km
Initial upper crust width = 173 km
Initial upper crust thickness = 11 km
Initial middle/lower crust thickness = 21.5 km
Initial crustal thickness 32.5 km
Present-day crustal width (middle-lower crust width) = 226 km
Initial crustal width = 174 km
Extension WC = 52 km
Area continental crust = 5657 km²
Area upper crust = 1900 km²
Area middle-lower crust = 3757 km²
0
40 km
50 km
South Florida
Initial middle-lower crust width = 256.5 km
Initial upper crust width = 266.5 km
Initial upper crust thickness = 11 km
Initial middle/lower crust thickness = 22 km
Initial crustal thickness 33 km
Present-day crustal width (middle-lower crust width) = 335 km
Initial crustal width = 265 km
Extension WC = 70 km
Area continental crust = 8701 km²
Area upper crust = 2932 km²
Area middle-lower crust = 5769 km²
0
40 km
b) Central cross-section
Central Yucatan
Initial middle-lower crust width = 194.5 km
Initial upper crust width = 187 km
Initial upper crust thickness = 10.5 km
Initial middle/lower crust thickness = 21 km
Initial crustal thickness 31.5 km
Present-day crustal width (middle-lower crust width) = 293 km
Initial crustal width = 192 km
Extension WC = 101 km
Area continental crust = 6045 km²
Area upper crust = 1961 km²
Area middle-lower crust = 4084 km²
0
40 km
50 km
North Florida
Area continental crust = 5900 km²
Initial crustal thickness 34 km
Present-day crustal width (middle-lower crust width) = 314 km
Initial crustal width = 173.5 km
Extension WC = 140.5 km
0
40 km
c) Western cross-section
West Yucatan
Initial middle-lower crust width = 186 km
Initial upper crust width = 193 km
Initial upper crust thickness = 11 km
Initial middle/lower crust thickness = 20 km
Initial crustal thickness 31 km
Present-day crustal width (middle-lower crust width) = 299km
Initial crustal width = 188.5 km
Extension WC = 110.5 km
Area continental crust = 5844 km²
Area upper crust = 2122 km²
Area middle-lower crust = 3722 km²
0
40 km
50 km
Sea-bed
Base post-rift - Base Salt
Top Basement
Upper/middle-lower crust
Top Oceanic Crust
Continental Moho
Oceanic Moho
High Velocity Lower Crust
Eddy et al (2014)
Restored upper crust (pre-rift stages)
Restored lower crust (pre-rift stages)
Restored whole crust, WC (pre-rift stages)

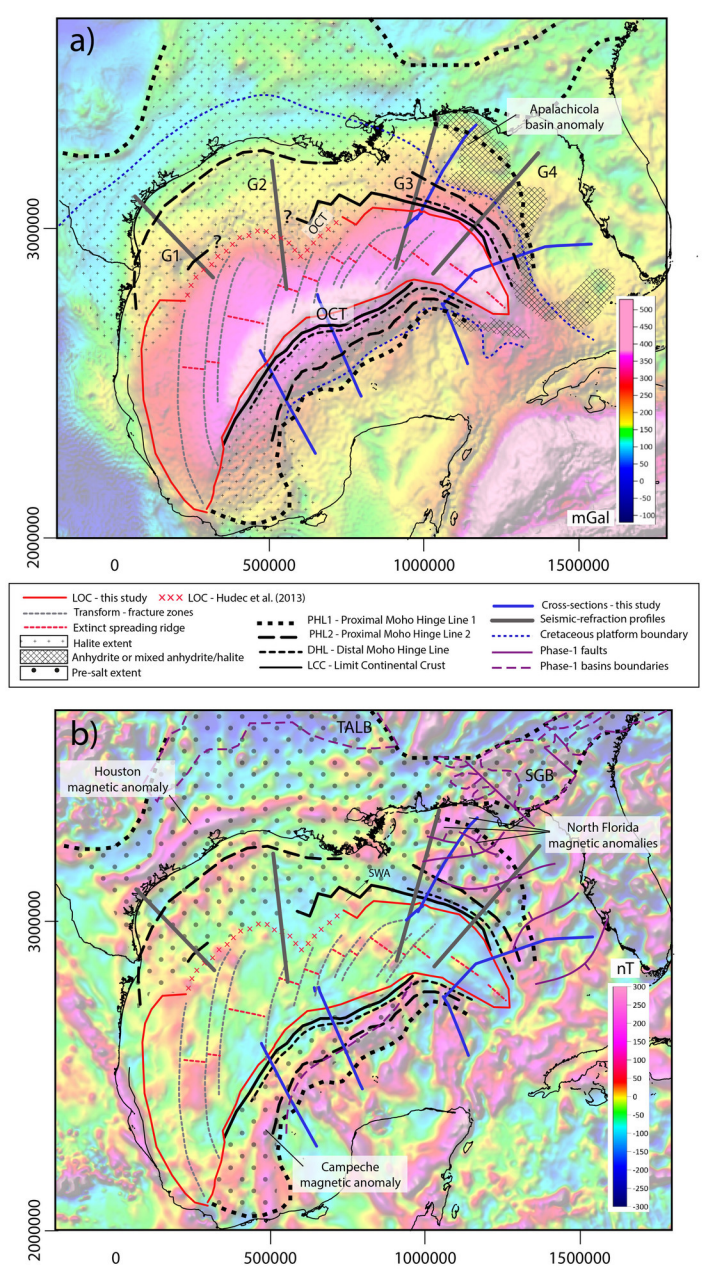
a)
Apalachicola basin anomaly
G1
G2
G3
G4
OCT
OCT
?
?
mGal
500
450
400
350
300
250
200
150
100
50
0
-50
-100
3000000
2000000
0
500000
1000000
1500000
LOC - this study
LOC - Hudec et al. (2013)
Transform - fracture zones
Extinct spreading ridge
Halite extent
Anhydrite or mixed anhydrite/halite
Pre-salt extent
PHL1 - Proximal Moho Hinge Line 1
PHL2 - Proximal Moho Hinge Line 2
DHL - Distal Moho Hinge Line
LCC - Limit Continental Crust
Cross-sections - this study
Seismic-refraction profiles
Cretaceous platform boundary
Phase-1 faults
Phase-1 basins boundaries
b)
TALB
SGB
Houston magnetic anomaly
North Florida magnetic anomalies
SWA
Campeche magnetic anomaly
nT
300
250
200
150
100
50
0
-50
-100
-150
-200
-250
-300
3000000
2000000
0
500000
1000000
1500000

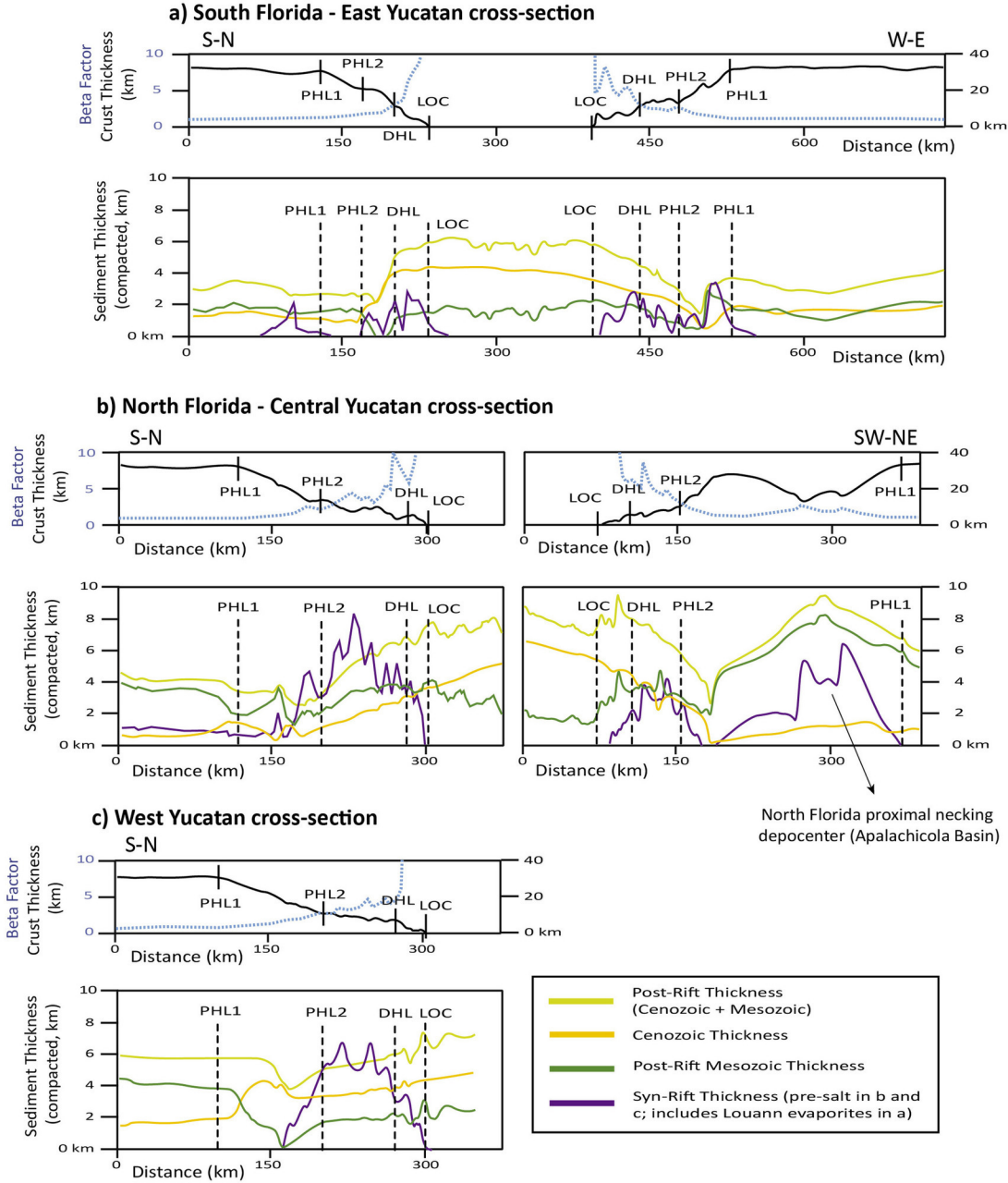
a) South Florida - East Yucatan cross-section
S-N
W-E
Beta Factor
Crust Thickness (km)
PHL1
PHL2
DHL
LOC
Distance (km)
Sediment Thickness (compacted, km)
b) North Florida - Central Yucatan cross-section
SW-NE
North Florida proximal necking depocenter (Apalachicola Basin)
c) West Yucatan cross-section
Post-Rift Thickness (Cenozoic + Mesozoic)
Cenozoic Thickness
Post-Rift Mesozoic Thickness
Syn-Rift Thickness (pre-salt in b and c; includes Louann evaporites in a)

A) NORTH FLORIDA AND CENTRAL-WESTERN YUCATAN

1) 1st rifting stage - Late Triassic - Early Jurassic. Early rifting involving magmatism.

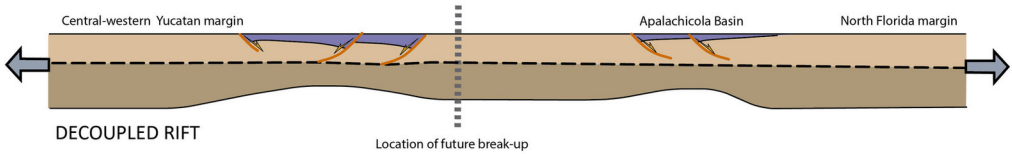

2) 2nd rifting stage - Early-Middle Jurassic. Magma-poor margin.

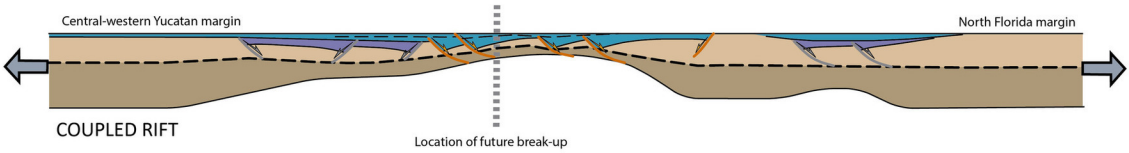

3) 3rd rifting stage - Bajocian - Callovian. Mantle exhumation and moderate magmatism at the OCT.

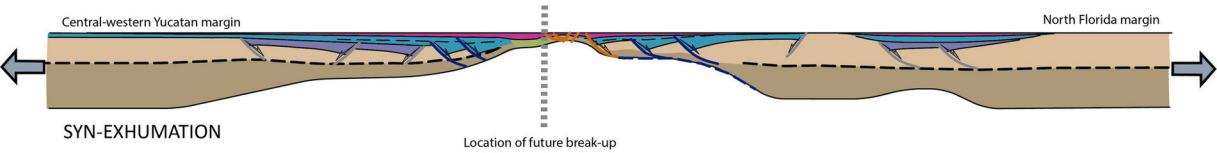

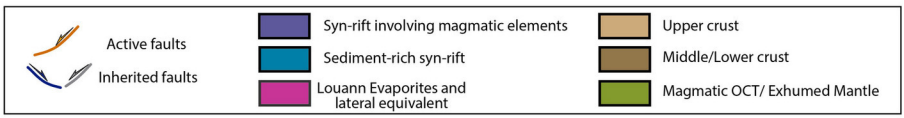

B) SOUTH FLORIDA AND EASTERN YUCATAN

3) 1st rifting stage - Bajocian - Callovian. Syn-rift deposition (lateral equivalent of the Louann Salt)

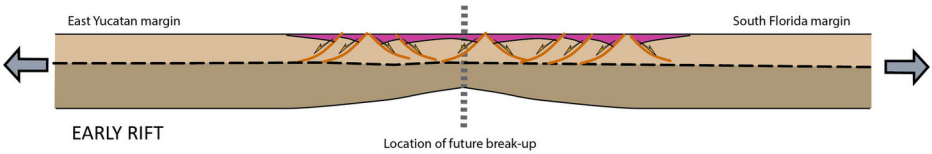

4) 2nd rifting stage - Oxfordian.